Design of Optical Measurements for Electrothermal Plasma Discharges

Matthew David Hamer

Thesis submitted to the faculty of the Virginia Polytechnic Institute and State University in partial fulfillment of the requirements for the degree of

Master of Science

In

Mechanical Engineering

Leigh Winfrey

Mark A. Pierson

Bahareh Behkam

May 2nd, 2014

Blacksburg, Virginia

Keywords: Electrothermal plasma, plasma diagnostics, spectroscopy, high speed imaging, high resolution spectrometer, Lexan, electron temperature, electron density, plasma jet velocity.

Design of Optical Measurements for Electrothermal Plasma Discharges

Matthew David Hamer

ABSTRACT

Ablation controlled electrothermal (ET) plasma discharge devices consist of a small diameter capillary through which a large amount of energy is discharged. The high energy in the discharge ablates an inner sleeve material, ionizes the material, and a high energy-density plasma jet accelerates out the open end. ET devices can find applications in internal combustion engines, Tokamak fusion fueling and stabilization, hypervelocity launchers, and propulsion. The ballistic properties of an ET device are highly dependent on the propellant and ablated material. A useful noninvasive technique to characterize a propellant in these types of devices is spectroscopy. The purpose of this study is to design and conduct experiments on the ET facility called PIPE to verify results and assumptions in the ETFLOW simulation code as well as resolve data collection issues such as equipment triggering as spectrometer saturation. Experiments are carried out using an Ocean Optics LIBS2500plus high resolution spectrometer and a Photron FASTCAM SA4 high speed camera. Electron plasma temperatures are estimated using copper peaks in the UV region with the relative line intensity method, and electron plasma density is estimated by measuring the full width at half maximum (FWHM) of the stark broadened H-β line at 486 nm. Electron temperatures between 0.19 eV and 0.49 eV, and electron densities between $4.68*10^{22}$ m^{-3} and $5.75*10^{22}$ m^{-3} were measured in the expanding plasma jet about an inch outside the source with values as expected for this region. Velocity measurements of PIPE match well with simulations at around 5333 m/s. This study concluded that the assumption that the propellant Lexan is completely dissociated is a valid assumption, and that the ETFLOW results for electron temperature, density, and bulk plasma velocity match experimental values.

Dedication

I would like to dedicate this work to my family and Julianne. My family has always blessed me with love. Their constant support and encouragement throughout my life and college career have brought me to where I am today. Julianne's love and belief in me constantly inspires me to do better than ever before.

Acknowledgements

I would like to first acknowledge Dr. Leigh Winfrey for teaching me so much in the area of plasma science and giving me the opportunity to be part of such exciting research. Dr. Mark Pierson has been a teacher and advisor of my nuclear studies at Virginia Tech for many years now and is responsible for helping me discover my passion for nuclear science. Dr. Bahareh Behkam has been one of the most inspiring teachers I have had at Virginia Tech. I would like to acknowledge Dr. Mohamed Bourham for his contributing discussions, and assistance with the use of the PIPE device at North Carolina State University. I would also like to thank my lab group for all their useful discussions, and Dr. Yang Liu for contributing high speed camera equipment to conduct part of this research. All photos by author, 2014.

Table of Contents

List of figures

Chapter 1: Introduction

1.1 Project Introduction

Ablation-dominated electrothermal (ET) plasmas are high-density low-temperature plasmas. They are generated in small diameter capillaries with removable ablative liners. A high energy pulse from a capacitor is discharged through the capillary to generate the high energy-density plasma and subsequent high velocity plasma jet. Plasma diagnostics is an important topic of study in the field of high density electrothermal (ET) plasma discharges. Electrothermal plasma devices have many applications such as fusion fueling [16-17, 19], thruster propulsion [24, 34-35], supersonic flow control [1], materials deposition [11], projectile launchers [5], and assisted internal combustion engines [2]. As with any engineered system ET devices must be tested before they can be used commercially. ET discharge systems are simulated using computer models to get theoretical values, such as temperature, density, and velocity of the plasma to see how the plasma acts under different formation conditions. These systems are further tested by building experiments which operate under conditions that would be near that of commercial use. Diagnostic tools are used on the experiment to see whether it does or does not match the computer simulations. These tools measure parameters such as density, temperature, and velocity of the experimental plasma to compare it to the simulated plasma. It is important to validate experimental results to understand if the experiment, in reality, will perform the way it does theoretically and vice versa.

This research focuses on the diagnostics of electrothermal plasmas by means of spectroscopy and a high speed camera. Spectroscopy of plasma in this research is conducted using high resolution spectrometers. Collected spectra are used to determine density and temperature of the plasma. The high speed camera provides a velocity profile of the plasma

plume as it leaves the ET source. The electrothermal discharge device used for this research is the Plasma Interaction with Propellant Experiment (PIPE) at North Carolina State University [3].

The purpose of this research is to verify electrothermal plasma simulation results by comparing current simulation parameters with current experimental parameters, specifically, density, temperature, velocity, and dissociation. This study also serves to find solutions to the spectrometer saturation and triggering issues. The current computer code used to simulate the ET plasmas is called ETFLOW. Past results for similar experiments have shown plasma densities on the order of 10^{23} - 10^{24} m^3 and plasma temperatures around 1.2 - 2.4 eV using optical emission spectroscopy (OES) [8-9]. These measurements were made on PIPE to compare to the simulation code ETFLOW, which returned results for plasma density between 10^{24} - 10^{26} m^3 and plasma temperature between 1 - 3 eV [3]. The results were similar for both density and temperature, but there is more of a discrepancy in the density measurements. ETFLOW computes plasma velocities on the order of 4.5 - 6.2 kilometers per second for geometries similar to the experiment [3]. Velocity measurements have never been taken on PIPE. Experiments have been conducted on similar electrothermal plasma devices using break wire technology. These experiments were modeled by a computer code that predicted the results to within 15% of the pellet velocity [5]. Verifying the simulation plasma velocity with the experimental plasma velocity is an essential part of this study and will provide new insights into these types of plasmas.

This chapter focuses on the purpose of this research, the basics of plasmas and ET devices, and provides an analysis of past work in plasma diagnostics. An analysis of past work will illuminate areas of research that need more attention as well as unanswered questions that this research strives to answer. Chapter 2 explains the details of the experimental method,

specifications of the tools used, and the procedure for collecting and processing data. Chapter 3 presents the results of the study and a discussion thereof. Finally, chapter 4 concludes this study and describes future work that will come from the research presented in this thesis.

1.2 Introduction to Plasmas

Plasma is not a solid, liquid, or gas. It is considered a fourth state of matter. When energy is added to matter, in other words the temperature is increased, the energy of individual atoms in the matter goes up. When the energy of the atoms is high enough for them to collide together and knock off electrons then ionization occurs and a plasma is formed. Likewise, when energy addition is stopped the electrons and ions recombine and settle back down to a gas state. Ionization happens when an atom gains or loses electrons. Figure 1.1 depicts how an atom is ionized. Ionized gases, or plasmas, can be found all around us, fluorescent light bulbs, neon signs, stars, the auroras in our atmosphere, lightning, gaseous nebulas as well as most of the interstellar medium (most of our universe), and sparks to start your car engine, to name a few. Only a small percentage of a gas needs to be ionized in order for it to exhibit plasma behaviors. Ionization depends on multiple parameters, but plasma temperature is a main indicator [4].

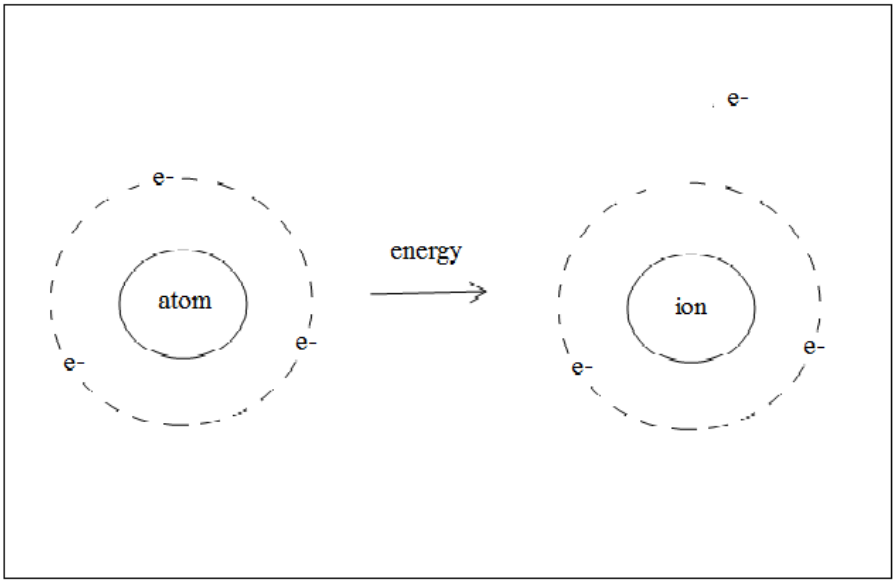

Figure 1.1: Ionization happens when enough energy is added to an atom and collisions between molecules become great enough to overcome the binding energy of the outer electron and it breaks off from the atom. There is now an atom with a positive charge (ion) and a negative free electron.

Plasma temperature is a parameter that can be used to characterize and categorize plasma. An atom needs a certain amount of energy imparted to it to become ionized, so a measure of the energy is an indicator to the degree of ionization in the plasma. Temperature is nothing more than a measure of particle energy and plasma temperature is measured in electron volts (eV). One eV is equal to $1.602*10^{-19}$ Joules (J) or 11604.5 Kelvin (K) when divided by the Boltzmann constant in (J/K) [7]. To put these numbers into perspective, 11604.5 K or 1 eV is about twice the temperature of the surface of the sun. Plasma temperature is usually given in terms of the electron temperature rather than the ion temperature because electrons come into equilibrium first as they are much smaller particles. This is due to the difference in mass between electrons, ions, and neutral particles. Electrons are smaller than ions or atoms so in a collision between the two the electron will leave with more energy than the ion or atom. This is analogous to hitting a billiard ball (electron) with a bowling ball (ion or neutral). Electron temperatures around 1 eV

have been estimated on the ET experiment used in this research by means of OES and the emission lines of copper [8]. Similar experiments were conducted on other ET plasma facilities which yielded temperatures between 1-2 eV [9]. Movement of electrons and ions not only allows one to estimate the temperature of plasma, but it also makes the plasma electrically conductive.

Plasma is different from gas because it is electrically conductive, and therefore there are interactions between charged particles and electric fields that do not occur in gases. What makes plasma electrically conductive is the mobile electrons and ions that can carry charge through the medium [4]. As discussed earlier, when the atoms in a gas are heated up enough to ionize then there is a certain number of free electrons, ions, and neutral particles in the plasma. The electrons and ions move through the plasma carrying charge with them. However, as a whole, plasmas are electrically neutral because the positive charges and negative charges cancel each other out. The electron density (n_e), ion density (n_i), and neutral density (n_o) make up the total density of the plasma (n), and is usually measured in n/m^3 or n/cm^3. Quasi-neutrality happens when the density of electrons, ions, and neutrals is the same so that the bulk charge of the plasma is zero, $n_e = n_i = n_o$. It is important to remember that in many cases the plasma is not in equilibrium. There are regions of higher or lower density, molecules that did not dissociate, singly or doubly ionized atoms or molecules, and multiple species of atoms or molecules in the plasma [6]. In many applications, plasmas are assumed to be quasi-neutral with uniform density throughout to simplify calculations. These simplifying assumptions are applied in the ETFLOW code to model electrothermal plasma discharges like the device used in this research.

Another useful physical characteristic of plasmas is the Debye length (λ_D). Sometimes called the Debye radius or Debye sphere, this parameter is the distance away from a single

charged particle in a plasma over which the electrostatic field can be felt by other charged particles [4]. The Debye Sphere is essentially the measure of the size of the sphere of influence around an electron or ion. Other charged particles inside this sphere contribute and interact to the collective electric field, but charged particles that lie outside the sphere are screened and do not influence the fluctuation of charge within the sphere. For example, there is a positive ion with a certain size sphere around it. If there are enough electrons inside the Debye sphere to equal the positive charge on the ion then the ion is said to be completely screened, meaning the positive ion looks neutral to particles outside the sphere. High density ET plasmas, as are the subject of this study, are so dense that the Debye spheres of charged particles overlap and interfere with each other. This makes the plasma incompletely screened. Another factor that contributes to incomplete screening is the presence of neutral particles, seen in Figure 1.2 below. Using the example from above, neutrals may fill spaces inside the Debye sphere instead of electrons. In this case there may not be enough electrons inside the sphere to equal the charge of the positive ion. Incomplete screening happens because the particle does not look neutral to outside particles.

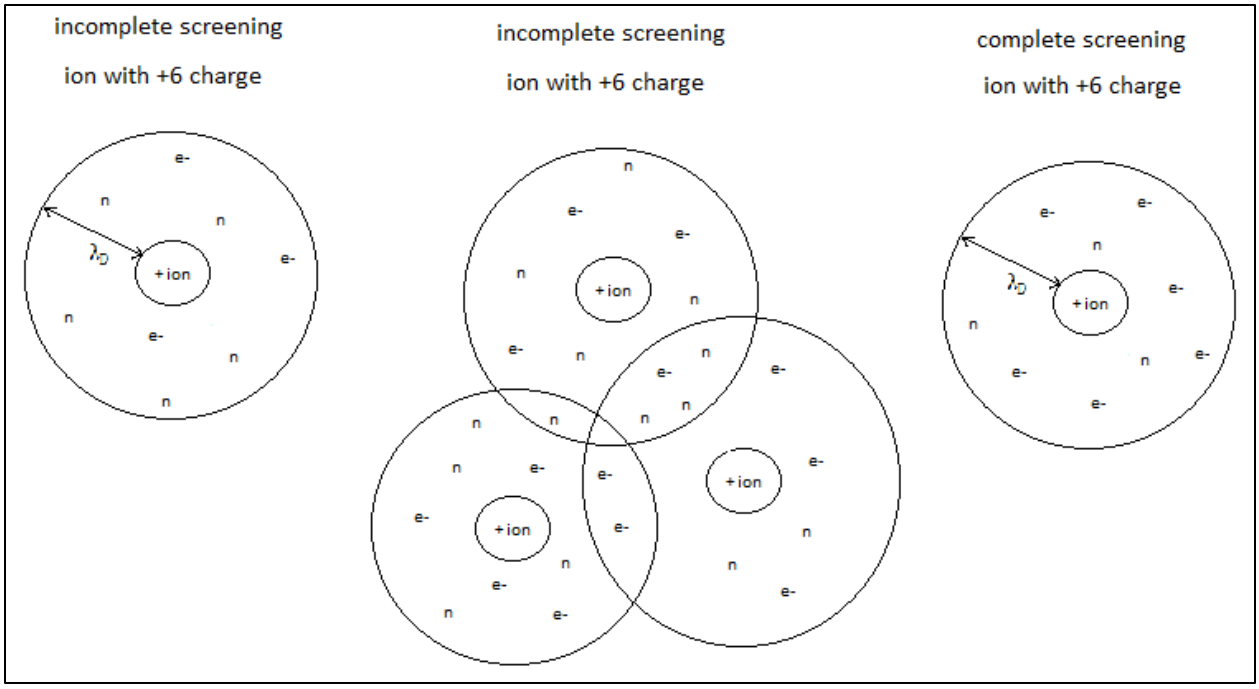

Figure 1.2: A completely screened ion with positive six charge that has six electrons within its Debye sphere will appear to have no charge to outside particles. However for screening to be incomplete the plasma may be dense enough for the Debye spheres of influence to overlap or have a high neutral count in the plasma. Too many neutral atoms will offset the charge balancing effect of the electrons.

Debye length, equation (1), is related to the temperature (T), in Kelvin, in this case electron temperature, and the electron density (n_e) in m^{-3}, both of which can be estimated through plasma spectroscopy [4].

$$\lambda_D = \left(\frac{\epsilon_o kT}{n_e e^2}\right)^{\frac{1}{2}} \quad (1)$$

ϵ_o is the permittivity of free space ($8.85*10^{-12}\ C^2/Nm^2$) [21], k is Boltzmann's constant ($1.38*10^{-23}\ Joule/K$, and e is the charge of an electron ($1.602*10^{-19}$ C) [4]. The Debye length is an important parameter when using electric probes for plasma diagnostics, discussed later in this chapter.

1.3 Electrothermal Plasma Discharge Devices

The test apparatus used to conduct this research employs a simple high voltage discharge system and spark-gap switch to generate a high-density, low-temperature plasma. The focus of this research is on the plasma plume once it exits the source. Spectroscopic measurements of the plasma formation inside the source have been attempted [9]. These measurements show hotter denser plasma inside the source with significant interference of emission measurements along the wall of the source due to boundary layer formation.

The ET system consists of a power supply, capacitors, spark-gap, trigger, source, vacuum chamber and vacuum pump. Figure 1.3 illustrates the overall schematic of the ET discharge system PIPE. The power supply charges a 340 μF capacitor to 1-5 kV which is discharged through the spark-gap switch when the system is triggered. The discharge current to the source is anywhere from 1-40 kA [3]. Voltage is measured with a capacitively coupled high-voltage probe and current is measured with a Pearson coil. The current profile is captured with an oscilloscope when the capacitors are discharged. The discharge current enters the source, creates a spark, ablates material, and a high pressure plasma is discharged out the open end of the source. The open end of the source is pumped down to approximately 50 mTorr to evacuate the plasma chamber of air. Creating a vacuum in the plasma chamber helps eliminate background interference when taking spectroscopic measurements. Otherwise, the air will interact with the important plasma-absorbing emission and fluorescence lines needed for spectral analysis.

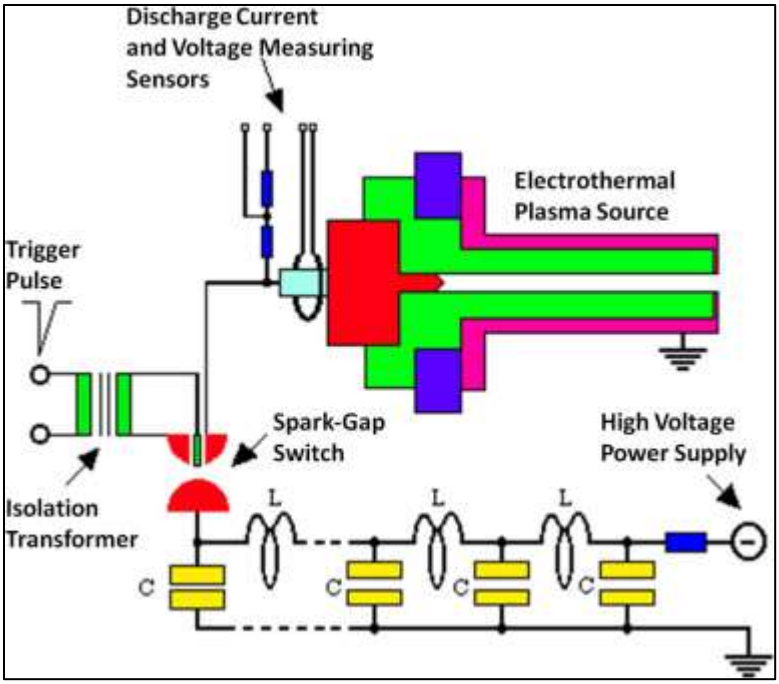

Figure 1.3: The electrothermal plasma discharge system uses a power supply to charge capacitors. The capacitors are triggered by an external trigger and discharged through a spark-gap switch. The high-current, high-voltage pulse enters the source and a spark is generated between the cathode and anode. This spark is hot enough to ablate off material from the inside wall of the source and accelerate it out the source into the vacuum chamber for spectroscopic measurement. A. L. Winfrey, et al. "A Study of Plasma Parameters in a Capillary Discharge With Calculations Using Ideal and Nonideal Plasma Models for Comparison With Experiment." IEEE Transactions on Plasma Science. 2012. Used under fair use, 2014.

The central piece to this system is the electrothermal source explained in Figure 1.4. The source is made up of a cathode, anode, and source liner. The cathode is a metal alloy rod, composed of 70% tungsten and 30% copper, rounded off at the end, and the anode is an oxygen-free brass alloy of 70% copper and 30% zinc. The cathode is nested into a cylindrical polycarbonate Lexan ablation sleeve. The Lexan ablation material is discussed in more detail in Section 1.4. The anode consists of a grounded brass housing that encapsulates the Lexan sleeve.

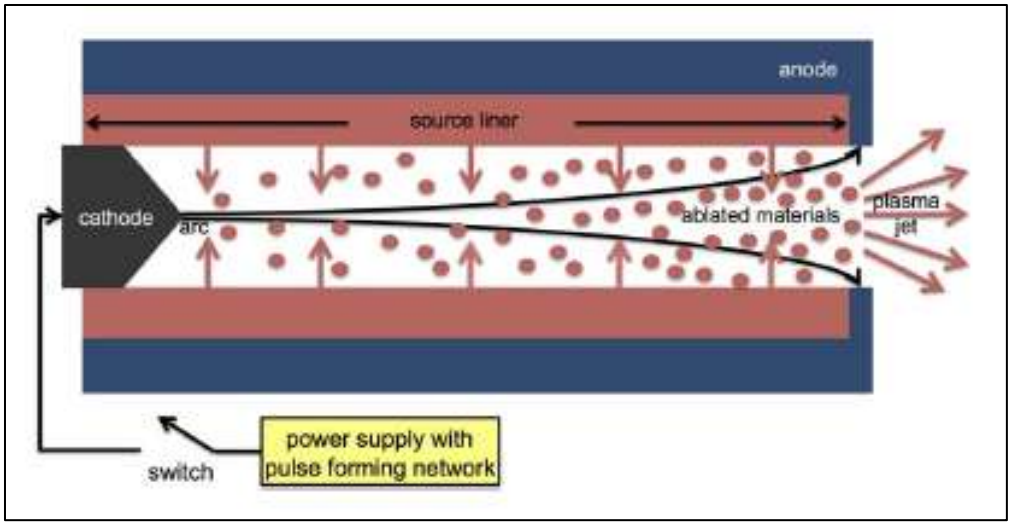

Figure 1.4: The source generates the electrothermal plasma by means of a high-current, high-voltage spark between the cathode and anode to radiate energy to the source liner and ablate off milligrams of the source liner material. There is a rapid increase in pressure inside the source and the ablated material is then accelerated out of the source. A. L. Winfrey, et al. "A Study of Plasma Parameters in a Capillary Discharge With Calculations Using Ideal and Nonideal Plasma Models for Comparison With Experiment." IEEE Transactions on Plasma Science. 2012. Used under fair use, 2014.

When the discharge current reaches the cathode a high energy spark is generated between the cathode and anode. The energy from the spark inside the Lexan sleeve radiates energy in the form of heat to the Lexan and ablates off material from the surface of the Lexan. The vaporized Lexan plasma increases the pressure inside the source liner, and exits the open end into the vacuum chamber. This process happens on the order of microseconds so the high pressure plasma exiting the source is moving at extremely high speeds. When the ET device is discharged it is referred to as a shot. The Lexan sleeve material can be substituted to study the effects of different materials and their erosion properties. Studies have been done with many metals and low atomic mass materials, however this study will incorporate the spectrometry of plasmas that include Lexan only. Figure 1.5 includes a picture of the assembled source on the PIPE experiment. The source is inside the cylindrical insulator. When the plasma enters the

vacuum chamber it is monitored by the spectrometer, through the fiber optic cable in the top of the chamber, and the high speed camera, through the quartz viewport in the front.

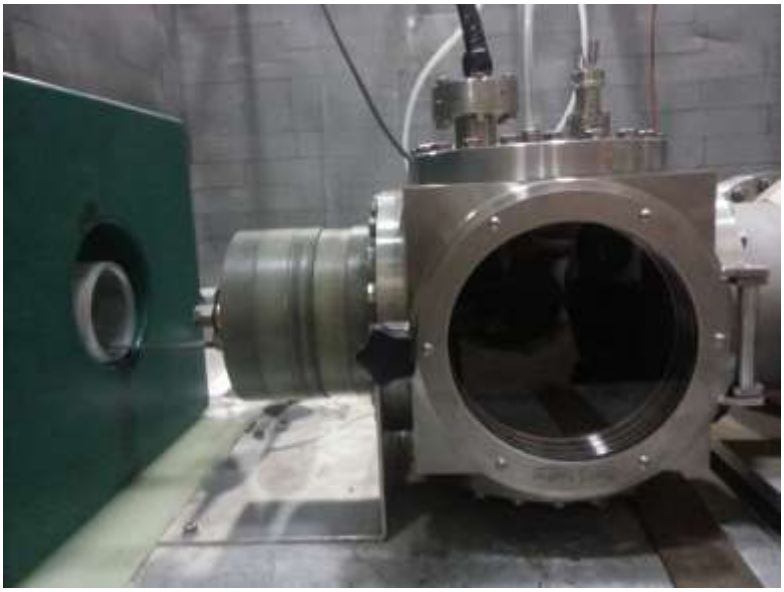

Figure 1.5: The electrothermal source is within the cylindrical insulator and bolted to the left side of the vacuum chamber to form a vacuum seal. It is bolted to the discharge power cable on the left, which passes through the Pearson coil to measure discharge current. The fiber optic cable for the spectrometer penetrates through the top of the chamber, and the quartz viewport in the front is for plasma viewing with the high speed camera

1.4 Ablation Sleeve Materials

Many Sleeve materials have been studied in ET ablation controlled experiments [11] [16-18]. Figure 1.6 shows how the sleeve material is arranged within the ablation source. Only Lexan was used in this study. No other ablation sleeve materials were inserted into the source. A discussion of the material used in this study is as follows.

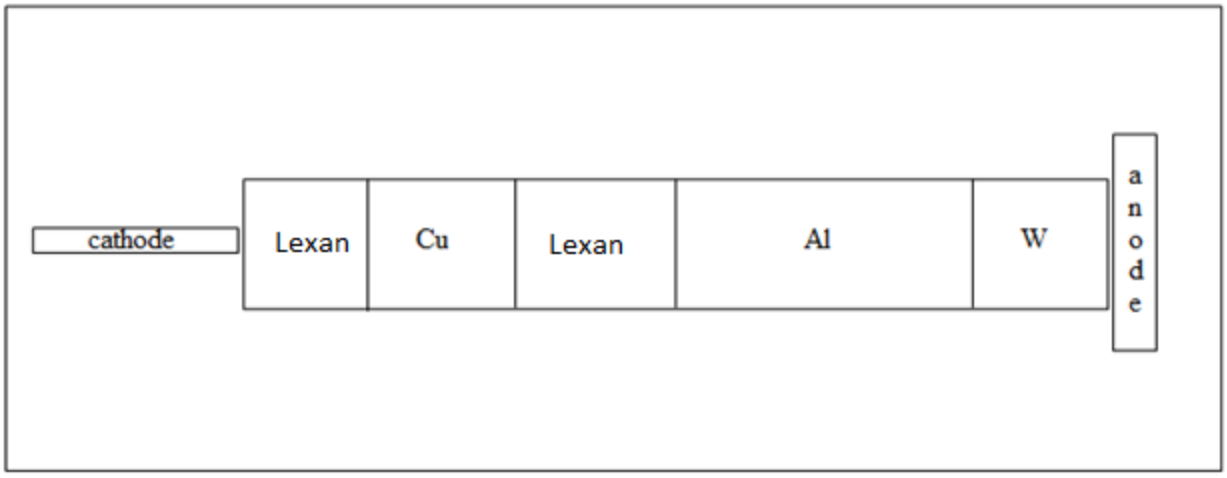

Figure 1.6: The ablation sleeve material is cylindrical in shape and hollow in order to slide into the insulator sleeve, and allow for the arc to pass from the cathode to the anode. Shots can be made of one material or many materials to study the interactions.

Metals are used in ET ablation experiments to simulate plasma disruptions and the effect of high heat flux on first wall materials in fusion reactors [16, 19-20]. However, this study was conducted with solely Lexan shots. Lexan has soot production properties similar to graphite which cannot be used in these experiments because it tends to shatter. Soot production is important for Tokamak reactors because carbon particulate tends to retain tritium and hydrogen which could buildup [16].

Lexan, $C_{16}H_{14}O_{3,}$ is a polycarbonate polymer [3]. Lexan is in the family of rigid plastics. It displays excellent properties over a wide temperature range. Lexan polycarbonate displays good transparency and resistance to solvents, impact, and creep, making it well suited for many applications [10]. A polymer is a chain of monomers formed together in the process of polymerization. Lexan is produced by reacting bisphenol A with phosgene. Polycarbonates are usually amorphous higher molecular weight polymers with long polymer chains. This makes them more rigid and gives them good mechanical properties [10]. There are synthetic polymers like Styrofoam, rubber, and PVC, and natural polymers like proteins, cellulose, and amino acids.

Lexan is used in these experiments to simulate materials that would be used in fusion reactors such as lithium deuteride or lithium hydride [11, 16]. Synthetic polymers were first developed in 1908 by Leo Hendrik Baekeland [12]. In the following decades intense research in the field of polymer chemistry led to the great number of techniques and materials that we use today. Coincidentally, during this same time period pioneering research in the field of plasma diagnostics was taking place.

1.5 Review of Literature and Plasma Diagnostic Techniques

The purpose of this section is to give an overview of methods that can be used to determine plasma parameters and characteristics. The methods are plasma probes, particle beams, microwaves, lasers, and spectroscopy. The focus will be on methods that determine density, temperature, dissociation, and velocity. This section will discuss the applicability of these methods to electrothermal plasma discharges and the experimental limitations with regard to the test setup in this research which led to the method of choice, i.e. optical and spectroscopic techniques.

1.5.1 Probe Diagnostic Method

Irving Langmuir first studied plasma in the early 1920's using electric probes to determine characteristics of plasma in a discharge tube [13]. There are many geometries, configurations, and methods for the use of probes in measuring plasma characteristics, but this section will focus on the single and double cylindrical probe methods [6] [13] [15]. The probe method is still rather popular today due to the simplicity of the setup. Analysis of plasma parameters can become difficult with dense plasma and magnetic field effects [13]. Probes have been used for many applications such as plasma etchers and ET thrusters [22-24]. The analysis

techniques used for probes assumes the plasma to be ideal, and it is known that the ET plasma in this study is weakly ideal.

A single unpolarized probe is the simplest method of probing plasma. These types of probes are called floating probes because they are not connected to a voltage source [6]. Probes are usually made of a conductive metal, in many cases simply an insulated wire inserted into the plasma. Measuring the induced current and voltage change on the floating probe allows one to determine plasma parameters. The length of probe exposed to the plasma will determine how much current is collected. When a probe is inserted into the plasma it will be hit by more electrons than ions, creating a negative voltage on the probe. The electrons begin to build up on the probe generating more negative current, but at the same time the ions are accelerated in the negative sheath region around the probe which increases the number of ions that hit the probe. Eventually, the number of both species hitting the probe will equal each other, and the probe will come to its floating potential [6]. Wherever charge separation occurs there is an induced electric field. At this point the current induced in the probe is negligible. Plasma parameters such as electron and ion density, electron temperature, and plasma potential can be determined from the recorded current voltage profile. Because this single probe method is limited to a few cases, double floating probes are used when there is not a reference electrode of known potential in the plasma, such as in electrodeless discharges [13].

The double probe setup uses identical probes in the plasma at a certain distance away from each other. These probes are connected to a variable voltage supply from which the voltage characteristic can be measured with respect to the plasma. Figure 1.7 shows a simple double floating probe circuit where V_a is the circuit voltage and I_s is the current in the circuit. The current drawn from the plasma in this regime must always be zero [13]. The equation that

describes this situation is a current balance where the ion current from probes one and two is equal to the electron current from probes one and two. For example, if probe one has a more positive voltage on it more electrons will be accelerated toward it and the electron current will be greater. This in turn will make a more negative voltage on probe two, accelerating ions toward it, increasing the ion current. The higher electron current in probe one and higher ion current in probe two cancel out to maintain an overall zero current. The overall zero current is an advantage over the single probe technique because the probes do not perturb the plasma by generating large sheath regions and affecting the natural flow of the plasma and fields within [6].

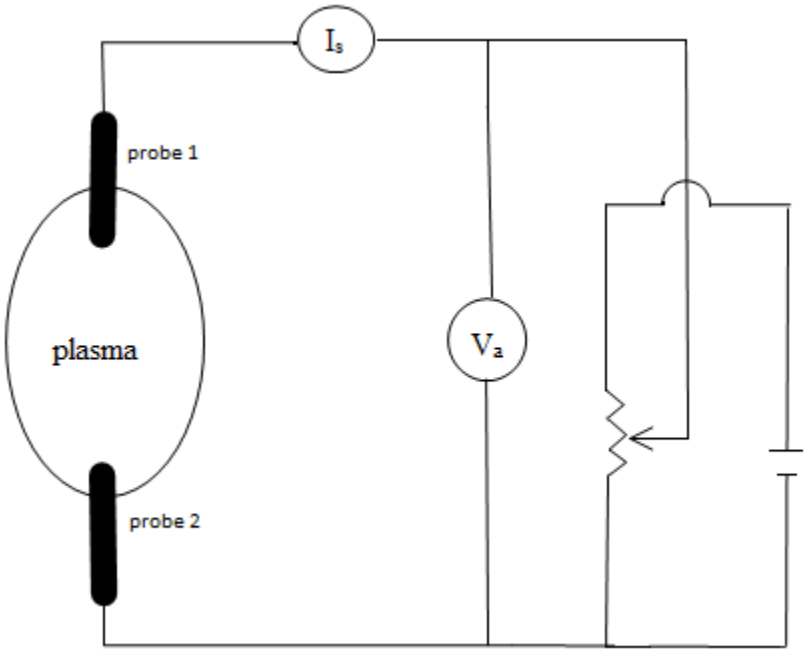

Figure 1.7: The double floating probe technique for defining plasma parameters requires that the sum of the ion and electron currents generated in the probes equals zero. V_a is the circuit voltage and I_s is the circuit current. J.D. Swift and M.J.R. Schwar. "Electrical Probes for Plasma Diagnostics" New York American Elsevier Publishing Company. Used under fair use, 2014.

Plasma perturbation is one reason for not using the probe method in this study. The plasma under scrutiny is discharged into a vacuum chamber which makes inserting physical

probes difficult. This is also a problem for developing a modular diagnostic system capable of being used on many experiments. Each experiment would need to be engineered to accept the probes for analysis. If in-bore measurements were needed then inserting a probe into the capillary would provide the high voltage discharge another path, possibly destroying the probe equipment in the process. The least invasive method possible to obtain undisturbed plasma measurements is required.

Langmuir probes are probes that have an applied voltage either across one or two probes. Depending on the experiment a two probe system may have any combination of biased or unbiased probes. As mentioned above, it is often desirable to have two probes to minimize plasma disturbance. Around the probes is a sheath region where the electric field generated in the probe dominates the behavior of charged particles. When the thickness of the sheath region is greater than the mean free path of the charged particles then Langmuir probes do not work. This is because the Debye radius, as discussed in section 1.2, must be much greater than the size of the probe. This puts a limit on the plasma temperature and density that probes can be used to measure. Probes can be easily used to measure plasma parameters as long as the plasma temperature does not exceed 20-30 eV and the density does not exceed $10^{14} – 10^{15}$ cm^{-3} [15]. The ET plasma in this study is on the order of 1-2 eV and 10^{23} m^{-3}, which is far too dense for easy probe parameter analysis. Magnetic or resonance probes can be used, but still require physical contact with the plasma [13]. The probe method for obtaining plasma parameters is a widely used technique, however it falls short when the experiment generates high density plasma, and requires a modular noninvasive method of analysis.

1.5.2 Particle Diagnostic Method

Particle diagnostic methods discussed in this section will cover electron, neutral, and ion beams that are directed into a plasma for diagnosing plasma parameters such as electric fields, magnetic fields, electron temperature, ionization fraction, density, plasma potential, or flow fields [14, 27, 32]. The physics of beam-plasma interaction is outside the scope of this study; however an overview of dominating interactions will be mentioned. Finally, particle beam diagnostic methods as they relate to the ET experiment in this study will be discussed.

Langmuir studied beam-plasma interactions during his work, but it did not become an important topic of study until a few decades later during massive research efforts in the area of nuclear weapons [15]. It was discovered that many of the observations that appeared in particle beam-plasma interactions were observed in thermonuclear experiments as well. Particle beam injection is conceptually simple. A beam of collimated ions or electrons is injected into an ionized plasma cloud. The beam can be continuous or pulsed to determine electric field line fluctuations. The beam is attenuated by interactions in the plasma and the exiting particle beam is collected and analyzed. The properties of the particle beam are known before it interacts with the plasma, so when it is collected on the other end, the change in the beam's composition or position carries information about the plasma density or induced fields [6].

Beam-plasma interaction is characterized not only by the particle-particle interactions within the ionized gas cloud, but with electric fields and magnetic fields within the plasma as well. This makes plasma beam-particle interactions complicated. Due to space charges and non-uniformities in plasma density the fields induced by charges within the plasma will be different

across the path of the beam. The different field strengths within the plasma will deflect the beam of charged particles, changing where the beam will strike the detector. The non-uniformities in the plasma make analysis difficult. Beams of neutrals can also be used to determine plasma parameters [25-26]. Neutral beams can be created by subjecting an ion beam to a magnetic field which will bend ions off course leaving a beam of neutrals [6]. Unlike ion or electron beams, the neutral beam will not be deflected by field fluctuations within the plasma. Neutral beams interact by means of charge exchange. Charge exchange is when a neutral in the beam swaps charges with an ion in the plasma. The neutral beam is contaminated with ions as it exits the plasma and impinges on the collector, and the amount of ion contamination in the exiting beam is a function of electron temperature and density, and density of the plasma [6] [15].

Other particle diagnostic methods include mass spectrometry and measurement of hard radiation emitted from the plasma. Neither of these methods would work on the ET system in this study because they both require deep vacuums on the order of 10^{-5} Torr to reduce error [15, 64]. The ET chamber in this study does not have this deep vacuum capability.

Particle diagnostic methods have an advantage over probe methods due to less plasma perturbation [15]. However in many cases the experimental setup can be extremely complicated and environmentally dependent. For proper collimation of electron beams the atmosphere must be pure and within certain pressures, and in many cases the experiment under scrutiny is already governed by another set of specific parameters [27]. For example, the vacuum chamber of the ET experiment in this study would need to be changed drastically from its current configuration to accept an electron beam, pure atmosphere, and high vacuum capabilities. Modularity of the particle beam diagnostic equipment is another issue for this study. In order for a particle beam to be used on multiple experiments it would need to be small, simple to set up, and easy to use,

none of which are properties inherent in particle beam diagnostic methods. Analysis of parameters using beam methods can be more complicated to interpret than probe methods and wave methods.

1.5.3 Wave Diagnostic Method

Waves propagate through plasma as they do through any fluid. Different interactions between waves and plasma make wave plasma diagnostics possible. This section will discuss diagnostic methods using microwaves, shock waves, and acoustic waves along with the parameters each method identifies. In high density, high velocity, small capillary ET experiments such as PIPE, microwaves do not propagate through the plasma and are much too noisy to measure plasma parameters [35-37]. Therefore, this paper will touch on the use of microwaves in plasmas, but will consider them for diagnostic use in this study.

When using microwave diagnostics the experiment is highly dependent on the frequency of the incident waves and the plasma frequency. Most importantly, if the microwave frequency is higher than the electron plasma frequency then microwaves will propagate through the plasma, but if the microwave frequency is smaller than the electron plasma frequency microwaves will be reflected [13]. If the plasma frequency is higher, plasma parameters are most often measured by a change in the microwave's phase, refractive index, or polarization [6, 28-29]. If the plasma frequency is lower, it is common to measure radiation emission from microwave excitation [6, 30-31]. Due to the dependence on frequency, it is possible to calibrate the microwaves to measure electron or ion frequency, which can be used to determine the temperature of each species. Microwave diagnostic methods fall short in measuring parameters in high velocity ET

plasma discharges, but microwaves are commonly used to generate plasma for plasma thruster applications [32-35].

The cavity perturbation method is classically applied to a discharge tube. The method begins with a cavity of known dimensions and a known frequency of microwaves. A plasma is then introduced into the cavity which will shift the frequency of the microwaves within the cavity [6, 13]. The frequency shift, or shift in the refractive index, is mathematically related to the plasma frequency and the electron density. The cavity perturbation method is accurate at measuring electron density of lower density plasmas.

Microwave interferometers can measure plasma density, electron temperature, or ion temperature [6, 13, 15]. A microwave generator sends calibrated waves down two parallel paths, one known, and the other with the unknown plasma. Along the known path the microwaves are attenuated and phase shifted so that they reach the detector side with the same phase lag and amplitude as the unknown plasma path [6]. Knowing the phase lag, microwave frequency, and plasma frequency one can determine density and temperature of the unknown plasma [13]. This technique has been used on ET plasma experiments to measure projectile velocity [38].

Shock waves are not used to measure plasma parameters, but they are used to generate high temperature plasma on the order of 10^6 K and 10^{16} cm^{-3} [6]. Other diagnostic techniques such as microwave interferometry or spectroscopy are used to determine plasma characteristics. The plasma is generated in the region in front of the shock where compression is enough such that the rise in temperature ionizes the working gas. Shock wave plasma is generated either by a physical diaphragm that bursts, or an electromagnetic discharge [6, 39-40].

Ion acoustic waves were first studied by Langmuir almost ninety years ago. Since then we have discovered that ion acoustic waves can be used to determine electron temperature, ion mass, ion concentration, and even drift velocity [41]. Ion acoustic waves are the plasma equivalent of a sound wave in air. They are generated by the oscillation of ions in plasma. The equations of motion and dispersion through the plasma are explained well in [42]. This method of wave diagnostics has become more relevant in recent years with the high sensitivity due to lasers [43]. Observation of ion acoustic wave oscillation would be made difficult in ET plasma experiments due to high noise, plasma motion, and high density, but the study of acoustic waves generated by the discharge in this research would an interesting topic of study.

1.5.4 Laser Diagnostic Method

As described above, microwave interferometry for plasma diagnostics works until the plasma is too dense for penetration of microwaves. This was overcome with the advent of laser diagnostics in the 1960's. Lasers are monochromatic beams of photons that allow for diagnostics of plasmas at much higher densities [15]. Today's lasers have even higher collimation, coherence, and power density which allows for extremely precise tunability of diagnostic experiments. In diagnostics, lasers are mainly used to illuminate or fluoresce something in the field of study. The basics of fluorescence are discussed as well. Lasers can be used to determine species, temperature, density, velocity, ionization states, transition states, and dissociation. Lasers are so versatile because they can be continuous or pulsed, even down to femtosecond pulses, power and wavelength of the laser can be adjusted for the experiment, and optical equipment allows frequency adjustment and many configurations. Lasers can also be used to generate plasma [44-46]. Lasers are the most state of the art in diagnostics. The generated plasma is characterized through emission spectroscopy, discussed in the next section.

This section will discuss techniques used for laser diagnostics, and their possible application to electrothermal discharge experiments. Laser interferometry, Laser Doppler Velocimetry (LDV), Particle Image Velocimetry (PIV), and Laser Induced Fluorescence (LIF) are popular methods for determining plasma parameters and flow fields. Laser-based plasma diagnostic techniques work on the principles of collecting laser light or emission from the plasma to identify changes in the light.

Laser interferometry employs the same principals as microwave interferometry, but with a laser beam [6, 13, 15]. The laser beam can be split down two paths, however with lasers the experiment can be simplified to a single path with the laser passing through the plasma and into the detection system. Laser interferometry is used to measure electron density and temperature precisely through the refractive index of a plasma or the Doppler shift in the laser as it interacts with the electrons in the plasma. Laser techniques are more suitable for high electron density plasmas for this reason [13]. Many configurations for the interferometer exist. Another advantage of laser diagnostics is the ability to characterize plasmas moving at high speeds. LDV and PIV are great techniques for determining parameters of flowing plasma as well as conventional flows.

LDV and PIV will be lumped together for this discussion. This is because LDV and PIV are similar in operation and visualization of flow fields. They both rely on reflection of laser light from seeding particles in the flow to visualize changes in particle motion over a short time period. Although these two techniques are based in fluid mechanics they have been used in plasma applications [47-49]. In both techniques reflective particles are introduced into the flow. It is important for the seed particles to closely represent the bulk particles in the fluid so that the seed particles accurately represent and follow along with the natural flow of the fluid.

In Laser Doppler Velocimetry, a laser is usually split into two beams and the beams are crossed. The crossed laser beams must match in characteristics and polarization, so it is easiest to use one laser. The intersection point is in the flow field where the observer wants to measure particle velocity. When a seed particle passes through the intersection point it reflects laser light onto a detector. The reflected light will be doppler shifted because the particle is in motion. The doppler shift of the reflected laser light is then a function of the reflection and laser beam angles, and light wavelengths [49-50].

When applied to electrothermal discharge experiments this technique has shortcomings. The seeding particles need to match the plasma in the flow field. This would prove difficult due to the fact that there are all manner of different sized particles as well as charges within the plasma interacting not only in bulk motion, but interacting with other high energy particles and electric fields. Introducing the seeding particles into the ablation controlled plasma would be difficult as well. The seed particles would need to either be injected somehow without interrupting the high voltage discharge, or imbedded into the ablation sleeve material. The high density of emission photons that come from the discharge would interfere with the reflected light, interfering with the doppler shift characteristics before it reaches the detector [15]. This is why doppler shift methods are not commonly used in moving plasmas. Also, LDV determines the velocity of a flow field at one point, but PIV can determine three dimensional velocity fields.

Particle Image Velocimetry, in its simplest setup, employs a thin laser sheet to illuminate a flow field which has reflective seeding particles in it. A high speed camera is triggered to take snapshots at the same time as laser pulses so that the images can be processed to get velocity vectors. To obtain three dimensional flow fields PIV uses multiple lasers and multiple cameras

or one laser and multiple cameras. These methods are called stereoscopic PIV or tomographic PIV [51-52].

The problems with using PIV on electrothermal discharges are similar to that of LDV. Optical noise, collisional quenching, and other interference between the reflected light and emitted light make flow determination difficult. These effects can be reduced with optical filters and polarizers, however, in the case of electrothermal discharges; a laser is not needed to illuminate the flow because the discharge is already illuminated by emission from the plasma plume. This renders PIV unnecessary. Solely a high speed camera can be used to visualize plasma flow in this case. That is part of the focus of this study.

The above methods are focused on velocity measurements of plasma. PIV and LDV are expensive. Other simple reliable methods of plasma velocity measurement that could be used in ET discharge experiments are ballistic pendulums, spring loaded pendulums, or time of flight measurements [15]. Pendulums are simple, but invasive. Time of flight measurements using lasers, photomultipliers, or microwaves would not perturb the plasma as would physical probes [15]. High speed cameras were used in this study because of their ease of use, noninvasiveness, accuracy, and availability from Dr. Yang Liu and his Multiphase Flow and Thermal-hydraulics Laboratory (MFTL).

Laser Induced Fluorescence, sometimes called Laser Excited Atomic Fluorescence (LEAF), employs a laser at a certain wavelength to excite a selected transition in a certain atom or molecule to make it emit photons at a known wavelength. The photons are then collected with a detector. Fluorescence is essentially the emission of photons, but for something to fluoresce it must first absorb photons. Fluorescence is most easily understood in steps. One, something

absorbs a photon. When this happens it moves to a higher energy state, and it wants to return to a lower more stable energy state as soon as possible. Two, to do this it will emit a photon to return to a lower energy state. This process is illustrated in Figure 1.8. Fluorescence photons are generally emitted at slightly longer wavelengths than the exciting photons, but can be emitted at the same wavelength (resonance) or shorter wavelengths. This is because something will not emit all of the energy it absorbs. When something is excited it will not always release fluorescence photons. Fluorescence is a spontaneous emission and it has probabilities associated with it.

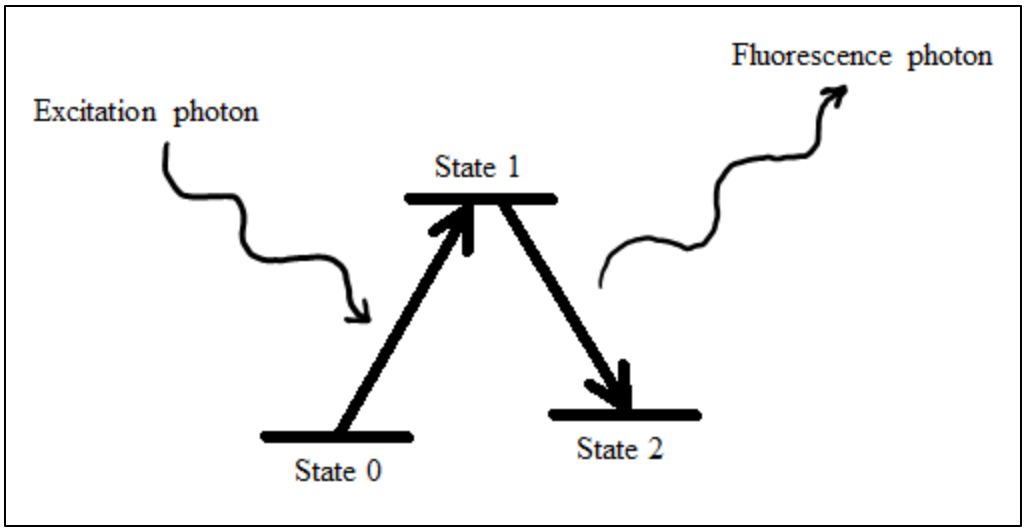

Figure 1.8: Fluorescence occurs when light is absorbed by something at state 0, exciting it to a higher energy level, state 1. To return to a lower energy level fluorescence light is emitted and it returns to a lower energy, state 2.

LIF is a versatile method of diagnostics used in many disciplines to study wastewater [53], biomedical [54], fuel injectors and combustion [55-57], plasma etching [58], tokamak fusion plasma [59], and electrothermal discharge devices [60-63]. LIF determines plasma parameters such as species concentration, electric fields, electron and ion temperatures, density, and velocity. This method works well for electrothermal capillary discharges because it is not as

sensitive to error as LDV. The laser is calibrated to fluoresce a transition to peak emission without saturating the transition, and then, because the fluorescence photon wavelength is known, an optical filter can reject most other photons except those around the fluorescence photon wavelength. That way the detector has the maximum probability of detecting the fluorescence photons. Lamps are commonly used in fluorescence and were used for decades before the invention of lasers.

1.5.5 Spectroscopic Diagnostic Method

When lasers or lamps are used to excite or illuminate a plasma, spectroscopic detection methods are often involved to capture the excitation photons or illuminated plasma. Spectroscopic techniques include photomultiplier tubes (PMT's), photography, spectrographs, photodiodes, and charge-coupled devices (CCD's). They are all used to detect the emitted light from plasmas. This section will discuss these methods, and how they have been used on ET discharge devices. The use of traditional photography, spectrographs in conjunction with multichannel analyzers, photodiodes, and PMT's are methods used on ET plasma devices, all of which were popular in the past [8-9, 18, 66, 68-69]. Research today has trended toward the use of CCD's, whether in spectrometers or high speed cameras [24, 44, 57, 63, 65, 67, 70]. CCD's are efficient for detecting photons over a wide spectral range, compact, cheap, and their use is seen in many new laser based diagnostic methods.

Ideally, the intensity of the emission from the bulk of the plasma is proportional to the square of the density, for high density plasma [15]. However, density measurements of ET plasma devices are complicated by emission from ionized species, neutral atoms, and secondary emissions. For these reasons, visual photography will not reveal all the information needed for

diagnostic work. Emission of the plasma in the visible wavelengths is a fraction of the emission from the whole plasma so photography can give a representation of the flow field, but cannot be relied upon for detailed emission measurements [6]. High speed digital cameras were not always available for time-resolved photography of ET plasma. High speed photography was limited by mechanical shutters speeds, which is much slower than the nanosecond order speeds required for use in ET devices [15]. Methods to get around this limitation use rotating mirrors, stroboscopes, or kerr cells to improve time resolution [6, 15]. Today's digital high speed cameras make it much easier to make time-resolved measurements of ET plasma. The high speed camera measurements in this study are discussed in Chapter 3. PMT's relay some of the same favorable characteristics as CCD's and have been used in studies on PIPE to obtain time resolved plasma measurements [18].

Spectroscopic diagnostics apply well to ET plasma discharge devices. Spectroscopy relies on the detection of photons emitted from the plasma so it is a completely noninvasive method of parameter detection. The modular high resolution spectrometers can easily be moved from experiment to experiment. No complicated setup and modification of experiments is needed to accept diagnostic equipment. Most importantly, spectroscopic diagnostics are capable of measuring the parameters of interest in this study.

This chapter has outlined many diagnostic methods for determining plasma parameters. From this overview it has been determined that some methods can be ruled out based on the criteria for this study. For this experiment the diagnostic system must be easy to use, modular, noninvasive, and cost effective. Plasma probes disturb the plasma so they are not used. Particle beam diagnostics can be eliminated due to the requirements of the experimental setup and lack of modularity. Microwave diagnostics is dependent on plasma frequency and refractive index, both

of which are complicated to determine in the transient high density ET plasmas. Laser diagnostics would work well for the ET device in this study; however, modularity, calibration, and cost are issues. This leads to spectroscopic diagnostics. Using spectroscopy is noninvasive, cost effective, does not require large scale experiment modification, modular, and easy for students and researchers alike to setup and take required data. Therefore, for this study, high speed cameras were used for velocity and flow measurements, xenon lamp fluorescence for plasma characterization, and high resolution spectrometers to obtain plasma parameters.

Chapter 2: Experimental Methods

This chapter explains the details of the experimental setup and methods of this research. Specifications of the high resolution spectrometers, high speed camera, and xenon flash lamp are discussed along with how they are integrated with the ET discharge device to collect data. The back end of the procedure is also explained. Spectral data is collected through OceanView software, and processed using SpecLine. This software is used to extract information on dissociation of Lexan, temperature, and density. The high speed camera software collects and processes images taken during each shot of the ET device to find bulk plasma velocity.

2.1 Equipment Specifications

An Ocean Optics LIBS2500plus high resolution spectrometer and Photron FASTCAM SA4 high speed camera collect optical data and send it to a laptop computer. The LIBS2500plus, shown in Figure 2.1 below, operates on a 5 volt power supply that plugs into a 110 volt wall outlet, and outputs data through a USB port. It has a resolution of around 0.1 nanometers with a wavelength range from 200-980 nm. It is made of seven HR2000+ high resolution spectrometers, each with a 2048-element CCD [71]. The seven spectrometers (channels) together are about the size of a shoebox. All channels are triggered to acquire data simultaneously with an integration time as low as 1 millisecond. High resolution is maintained in this system due to each of the seven channels having an operating range of around 100 nm. Light is collected through a single fiber optic cable and split into seven cables to connect to each channel.

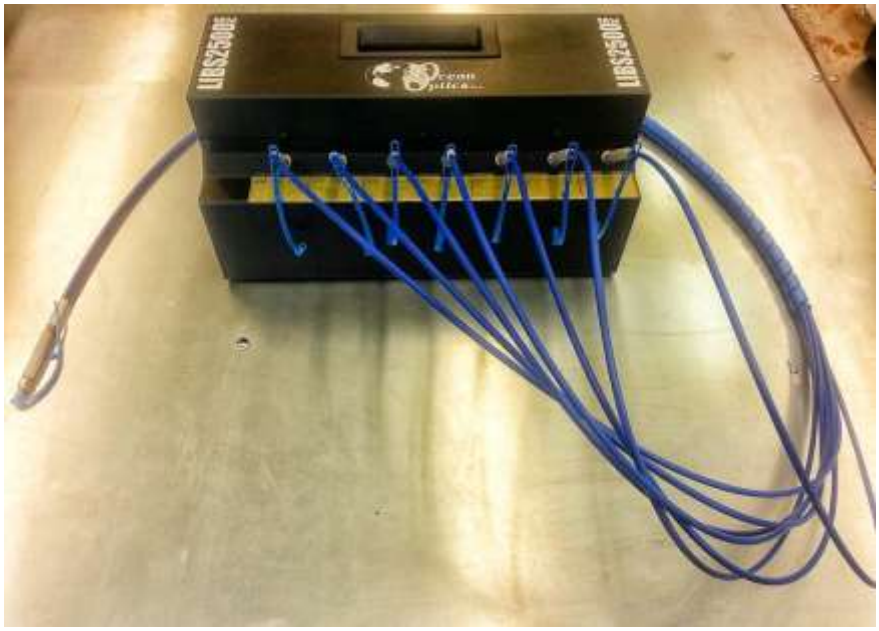

Figure 2.1: The LIBS2500plus high resolution spectrometer consists of seven HR2000+ spectrometers with 2048 element CCD's. With a resolution of 0.1 nm and wavelength range from 200-980 nm the spectrometer is designed specifically for plasma monitoring.

The LIBS2500plus is designed for plasma emission monitoring and detailed elemental detection down to parts per billion. The spectrometer is intended for use with a pulsed laser. When the laser is triggered by the spectrometer it ablates material off the sample target and creates a plasma. When the plasma cools emission lines are emitted by elements in the plasma and collected by the spectrometer. In this experiment the spectrometer is not used in conjunction with a laser, but in conjunction with an electrothermal plasma. This created triggering problems due to the fact that the spectrometer was not sending the triggering signal but receiving it. The solution to this problem is discussed in the next section.

The FASTCAM SA4 provides 1024x1024 resolution, 500,000 frames per second, and shutter speed capable of 1 microsecond. As the frame rate is increased the resolution of the saved images goes down. It is powered through a 24 volt DC power supply that plugs into a 110

volt wall outlet, and data is transferred via a gigabit Ethernet cable. The high speed camera has 8 gigabytes of memory onboard. The camera records until the memory fills, then the video can be saved to the computer in multiple formats. The aperture on the camera and the focus of any lens is adjusted manually. All other features and settings are adjusted in the Photron FASTCAM software.

2.2 Experimental Setup

This section explains how data collection tools are arranged around the research facility. A schematic of the overall experimental arrangement is first discussed, followed by detailed preparation of the high speed camera and spectrometer.

The experimental setup for this study is illustrated in Figure 2.2. The schematic does not show the vacuum pump and discharge network. The discharge network provides the power pulse to the source to generate the plasma. The plasma is discharged into the vacuum chamber, which is pumped down to around 15 mTorr. The high speed camera, xenon flash lamp, and fiber optic cable for the spectrometer, are all perpendicular to the plasma flow and ninety degrees offset from each other. In Figure 2.2 the spectrometer's fiber optic cable would be in the plane coming out of the paper. The discharge network current and voltage are monitored using an externally triggered oscilloscope. The high speed camera is triggered manually.

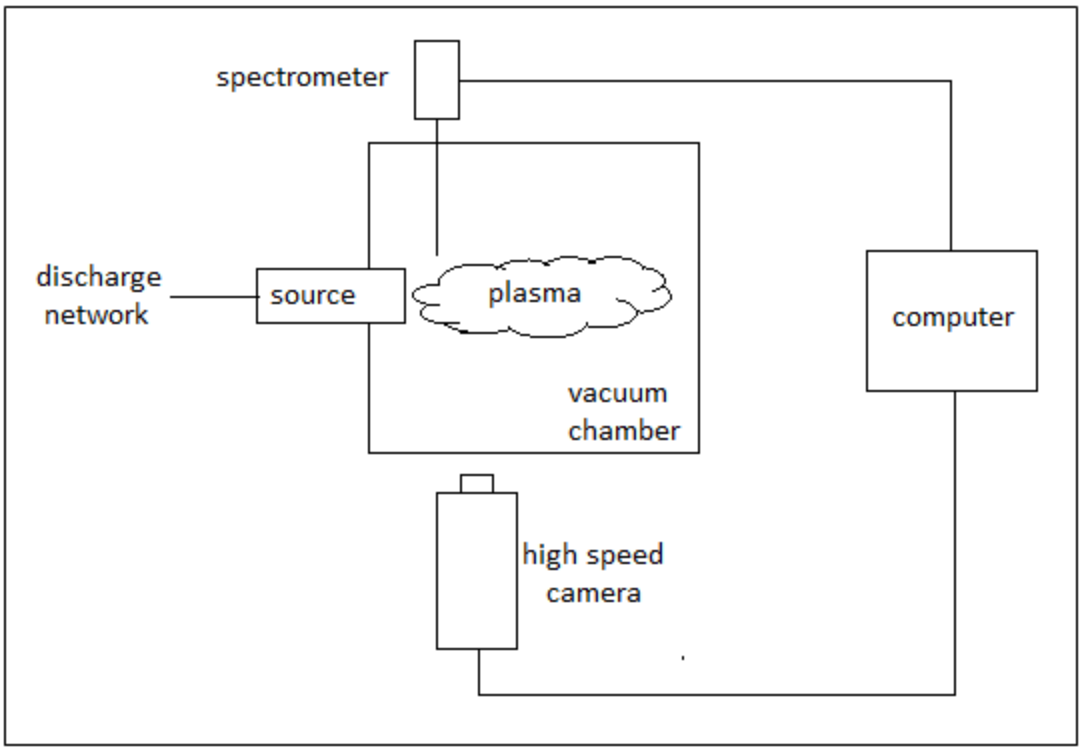

Figure 2.2: This schematic shows the experimental setup of the electrothermal discharge device without the vacuum pump or discharge network. In reality the optical fiber connected to the spectrometer is in the plane coming out of the paper to make the spectrometer, xenon flash lamp, and high speed camera ninety degrees offset from each other.

The Photron FASTCAM SA4 is mounted on a tripod so it is level with the plasma, as seen in Figure 2.3. The camera is kept at the maximum distance from the experiment, ground, and high voltage discharge system to isolate the electronics within the camera and reduce interference. Power cables and data cables are directed outside the discharge area when possible. A 180 millimeter lens is used at a focal length of about 33.25 inches to view the plasma plume once it exits the source through the eight inch viewport on the vacuum chamber. Videos recorded and stored on the camera are transferred and saved directly to the computer via the Ethernet cable. A lens cap is kept on and the camera is turned off at all times when the camera is not in use.

Figure 2.3: The FASTCAM SA4 high speed camera is mounted on a tripod to be level with the plasma plume as it exits the source. A 180 millimeter Nikon lens is used to obtain a close view of the ET discharge. The camera is placed away from the high voltage equipment to reduce electrical interference when in use.

The Ocean Optics LIBS2500plus spectrometer, shown in Figure 2.4, is operated outside the high voltage area. The fiber optic bundle is attached to the seven channels on the spectrometer and feeds through the penetration in the wall to the high voltage area. Figure 2.5 shows where the fiber bundle enters the high voltage area and is attached to the top of the vacuum chamber. Data is sent directly to the laptop via USB and saved on the computer hard drive for processing, which is discussed in the next section.

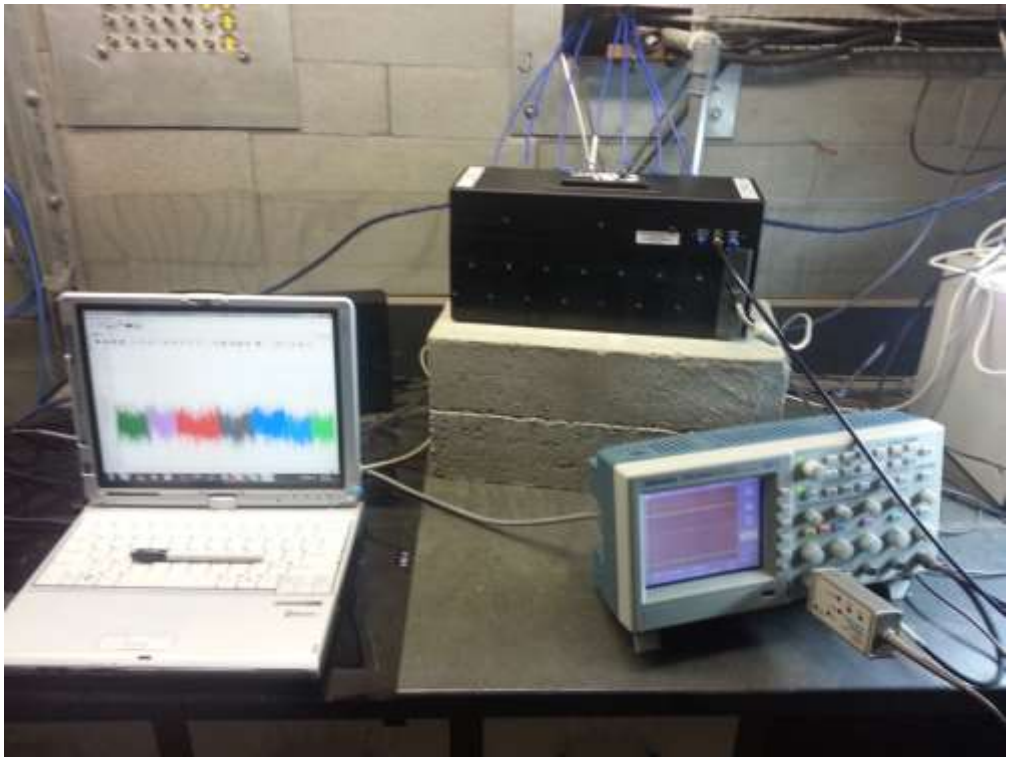

Figure 2.4: The LIBS2500plus spectrometer, oscilloscope, and laptop computer are separated from the high voltage side of the experiment by a concrete wall. The spectrometer fiber bundle passes through the wall and attaches to the top of the plasma vacuum chamber. Data collected from the spectrometer is saved directly to the computer through a USB port. The oscilloscope, front right, is used to record ET discharge current and voltage.

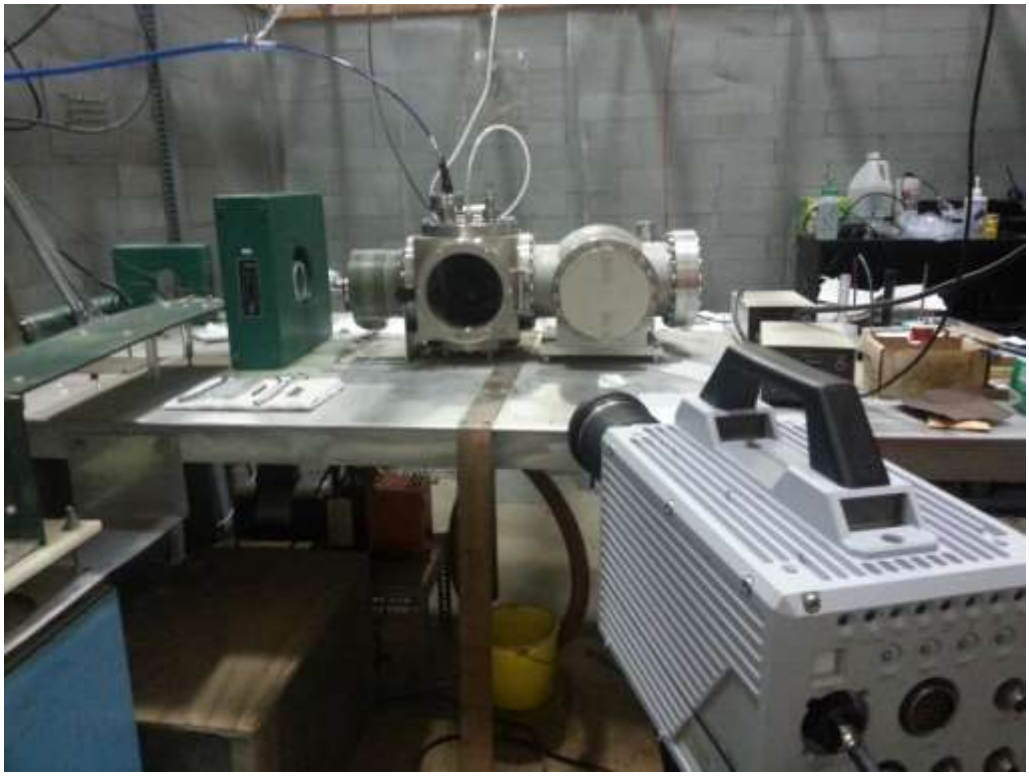

Figure 2.5: The blue fiber optic bundle from the spectrometer, top left, enters the top of the vacuum chamber. The plasma plume is recorded by the high speed camera, bottom right, through the viewport. Once charged, the capacitor in the bottom left of the picture is discharged to the source attached to the left of the chamber.

2.3 Data collection and Processing

This section discusses the collection and processing of optical information received from the spectrometer and high speed camera. Information from the spectrometer is collected in OceanView, compiled and graphed in Microsoft Excel®, and analyzed in SpecLine. Electron number density and temperature are estimated from the analyzed spectra. The high speed camera videos and images were processed in the Photron high speed camera software and the MATLAB® image processing toolbox.

2.3.1 Spectrum Collection in OceanView

OceanView is a general Ocean Optics spectrometer operating software. When a spectrometer is plugged into the computer, in this case the LIBS2500plus, it is automatically recognized when the software is opened. The user specifies the collection parameters and saves a background spectrum. A background spectrum is saved before each shot to subtract the background light from the Lexan shot to obtain the true emission line intensity. Integration time is an important parameter which is also controlled though OceanView. Integration time is the amount of time that the spectrometer collects light from the plasma. The lowest integration time possible for the LIBS2500plus is 1 ms, and is used to obtain the most time resolved spectra. The ideal time to collect emission from the plasma is after the initial bright flash of light. Elemental emission lines will be most prominent in the decline or cool down of the plasma plume. One important result from the high speed camera videos is the length of the bright flash. This information provides an estimate for the delay time to set the spectrometer to trigger in future experiments. The Lexan shot spectra collected in this study were saved as text files. The text files are in a two column format with wavelength, in nanometers, in the first column and counts in the second column (Figure 2.6). The text files are then imported to Excel for compiling and graphing.

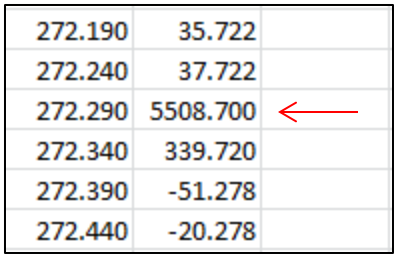

272.190	35.722
272.240	37.722
272.290	5508.700
272.340	339.720
272.390	-51.278
272.440	-20.278

Figure 2.6: OceanView saves spectra as text files in two columns. The left column is the wavelength is nanometers, and the right column is counts (relative intensity). Notice the clear peak at 272.29 nm.

2.3.2 Data Adjustment in Excel®

Excel is used to clean up the text files and graph the data from the spectrometers to view general trends. OceanView registers the LIBS2500plus spectrometer as seven different spectrometers. Data is saved in seven different files with a discontinuous range of wavelengths. This means there is an overlap in the ranges each spectrometer outputs to the text files. Text files must be spliced together continuously in order for SpecLine to properly identify peaks and elements. The spectrum saved by OceanView during each shot can be copied into Excel®, monotonized, and entered into a scatter plot. An example background spectrum from a Lexan shot is illustrated in Figure 2.7. The background spectra in this study are not dark. Peaks seen in the spectrum are from stray light entering from the eight inch viewport. SpecLine is used to subtract out the background from each shot.

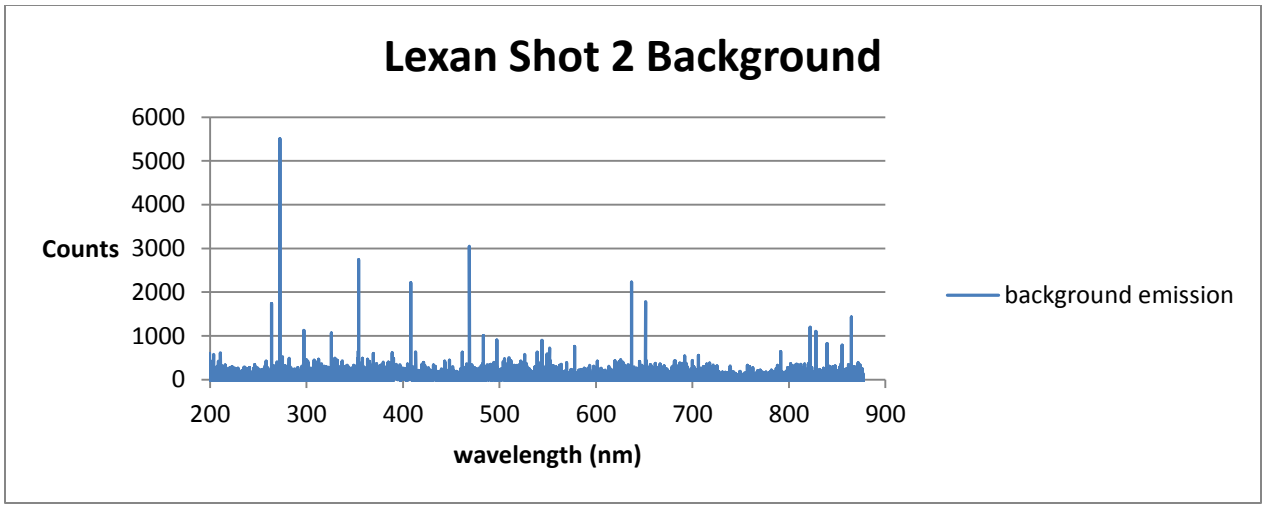

Figure 2.7: This background spectrum, created in Excel, has noticeable peaks from stray light outside of the vacuum chamber. This is due to the eight inch quartz viewport in the side of the chamber for the high speed camera.

2.3.3 Spectral Analysis with SpecLine

SpecLine is spectral analysis software developed in Germany and sold in the United States by Ocean Optics. It is a powerful analysis tool that allows multiple spectra to be compared and includes a large elemental and molecular database to automatically identify peaks and lines in a spectrum. Adjusted text files from OceanView can be imported directly into SpecLine. The background spectrum from a Lexan shot is subtracted from the actual Lexan shot so that only the Lexan shot is observed and analyzed. From the true uniform Lexan shot spectrum the peak finder and element identification tool is used to identify peaks from individual elements and molecular lines of interest. Lexan is made of mostly carbon, oxygen, and hydrogen, and the chamber is at a pressure of around 15 mTorr so there are still constituents of air to consider in the spectrum as well as the ablated material from the cathode and anode. All of these together should make up most of the emission lines viewed in the spectrum. The database in SpecLine is then adjusted to search the elements that may be in the plasma to save on

computation time. Identified peaks can then be used to estimate plasma number density and electron temperature.

2.3.4 Electron Plasma Temperature

Electron temperature is calculated using Lexan shot number two; two singly ionized copper peaks at 219.23 and 224.7 nm, shown in Figure 2.8; and the relative line intensity method. This method is valid to use as an approximation for ET plasmas in or near local thermodynamic equilibrium (LTE) of this temperature and density where electron temperatures are significantly higher than ion temperatures [3, 8-9, 11]. The error in using the relative line intensity method is usually greater than 10% [14]. For this method electron temperature is given by the following equation [11].

$$KT_e = \frac{E_{m1} - E_{m2}}{\ln\left(\frac{I_2\lambda_2^3}{I_1\lambda_1^3} * \frac{g_1 f_1}{g_2 f_2}\right)} \tag{2}$$

KT_e, the electron plasma temperature is in (eV). E_{m1} and E_{m2} are the upper level energy states of lines one and two in (eV). I_1 and I_2 are the intensities of the emitted lines in generic units of intensity. λ is the wavelength of the emitted lines in (nm). g_1 and g_2 are statistical weights of the upper levels of the emitted lines. f_1 and f_2 are oscillator strengths of the emitted lines. Equation (3) is used to find the oscillator strength where S is equal to the strength of the emitted line [72].

$$g_{1(2)} f_{12} = 303.8\lambda^{-1} S \tag{3}$$

Uncertainty in the electron temperature is calculated using uncertainties in variables taken from NIST, instrumental error in the intensity of measured peaks including the signal to noise ratio. Electron plasma density is measured using the stark broadened H-β line at 486 nm and tables

from (Gigosos and Cardenoso) to provide a secondary estimate of electron temperature and number density [73].

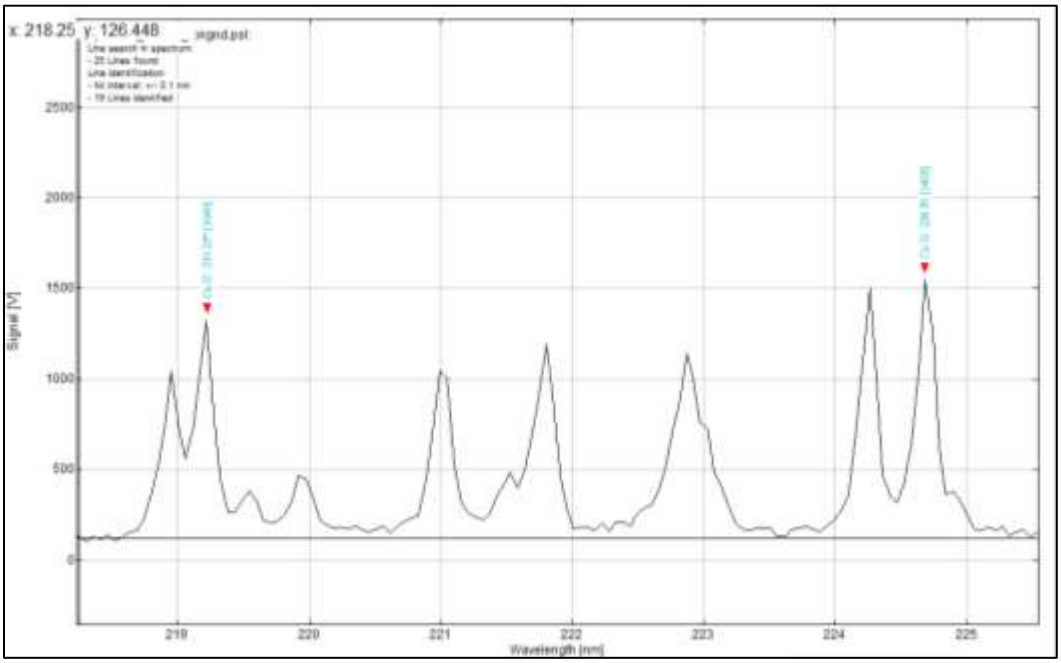

Figure 2.8: The two labeled peaks of singly ionized copper at 219.23 and 224.7 nm are used in the relative line intensity method to measure electron plasma temperature.

2.3.5 Electron Plasma Density

The spectrum of Lexan shot number two is used to estimate number density. The electron plasma density is estimated in two ways, both using the H-β line at 486 nm, illustrated in Figure 2.9. One method uses previously calculated tables, and the second uses the full width at half maximum (FWHM) of the H-β line with a Gaussian distribution function. To use the tables in (Gigosos and Cardenoso) the reduced mass (μ) is calculated using equation (4) [73].

$$\mu = \frac{1}{\frac{1}{m_e} + \frac{1}{m_H}} \tag{4}$$

m_e is the mass of an electron and m_H is the mass of a hydrogen ion (proton). The reduced mass is then normalized. With the reduced mass and the FWHM, calculated from the spectrum, the electron plasma density and temperature are found in the corresponding table. The FWHM of a Gaussian profile is given by

$$FWHM = 2\sqrt{2\ln 2} * \sigma \tag{5}$$

where σ is the standard deviation, and σ^2 would be the variance of the width of the profile. The estimated density is then expressed by

$$n_e = \left(\frac{FWHM}{FWHM_{measured}}\right) * 10^{23} \tag{6}$$

n_e is given in (m^{-3}) and $FWHM_{measured}$ is measured in the spectrum. The true FWHM is close to the measured FWHM if the ratio of the true FWHM to the spectral resolution of the spectrometer is greater than 3 [74]. Uncertainties are calculated using the instrumental error in measuring the FWHM, signal to noise ratio, and the variation in Gaussian profiles that fit the H-β line. Use of the Balmer series H-β line is very useful in this case because the line is little affected by self-absorption, plasma temperature, and ion dynamics [73]. If the density were measured by other lines in the spectrum ion effects would have a more significant effect given the many elements present.

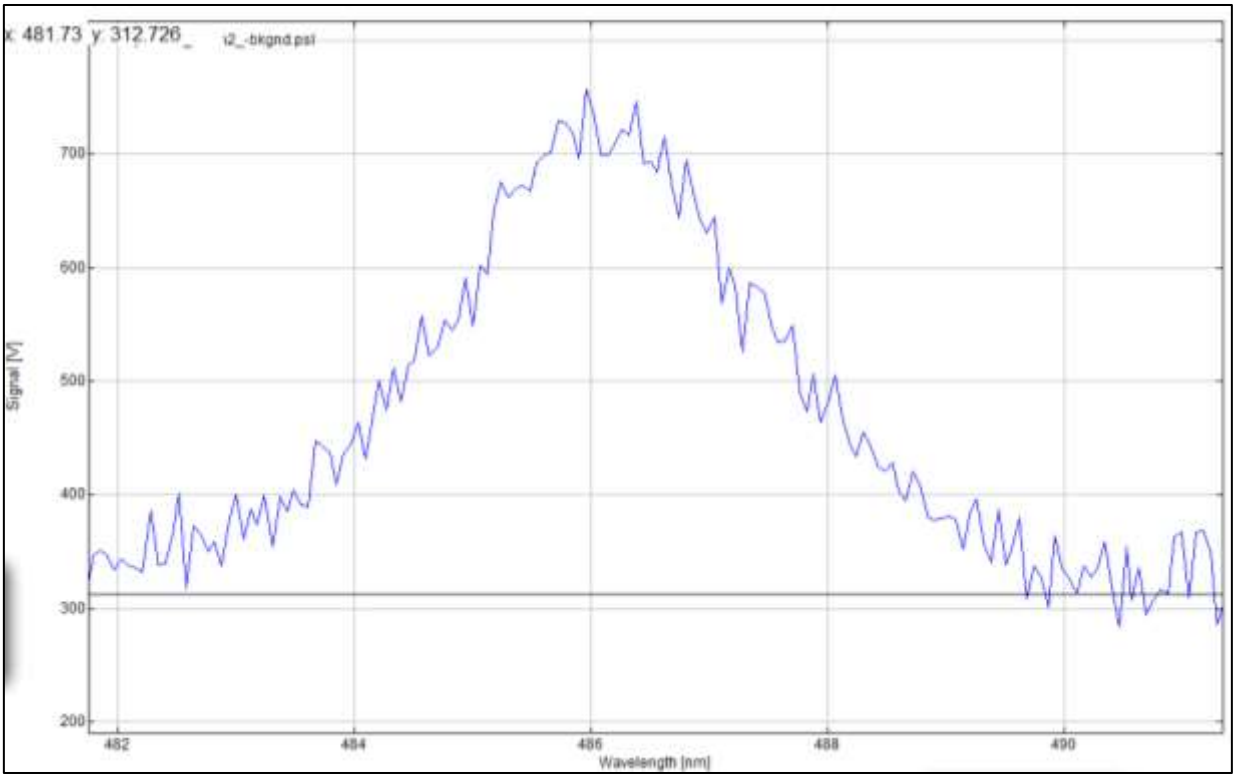

Figure 2.9: The Balmer series H-β line at 486 nm is used to estimate the plasma electron number density by measuring the FWHM of the peak. The H-β line is a useful stark broadened peak for density measurements in high density plasmas.

2.3.6 Velocity Measurements

Bulk plasma plume velocity information is retrieved from high speed videos for the purpose of comparing the experiment velocity with simulation velocity. The FASTCAM SA4 videos are processed directly in the Photron FASTCAM Viewer (PFV) software as well as post processing in MATLAB® image processing toolbox. The plasma velocity was calculated manually using images in PFV, and MATLAB® was used to validate the calculations and reduce calculation error.

Many shots were fired during these preliminary tests. It took multiple shots to configure the proper settings on the camera to capture the plasma jet. This left one video with usable

plasma data in it. The video data used to calculate bulk plasma velocity is from the third Lexan shot on the PIPE facility measured at 100,000 frames per second (fps). Lexan shot three was a 2.05 KJ shot with a discharge current and voltage of 17.7 KA and 3.03 KV. The energy of the shot is obtained by measuring the maximum voltage the capacitor is charged to and the residual charge left on the capacitor after discharge to the source. The voltage and current are measured by the oscilloscope, and transferred to a computer by USB drive. These numbers are important to record because they are used as input variables to the ETFLOW simulation code. For the purpose of this study the energy profile of the shot is important to compare to previously simulated shots in the same range to compare bulk plasma velocity.

Plasma velocity is calculated from a discontinuity in the visible plume in Lexan shot three. Figure 2.10 shows a frame by frame clip of the video where the plasma jet is clearly visible. The jet is expanding from left to right with the ET source on the left side of the images. The discontinuity is circled in black, and appears to move along with the plasma jet as it expands and dissipates. PFV has the tools to zoom in on a frame and measure distances between two points in separate frames. The velocity can then be calculated knowing the distance and time between frames.

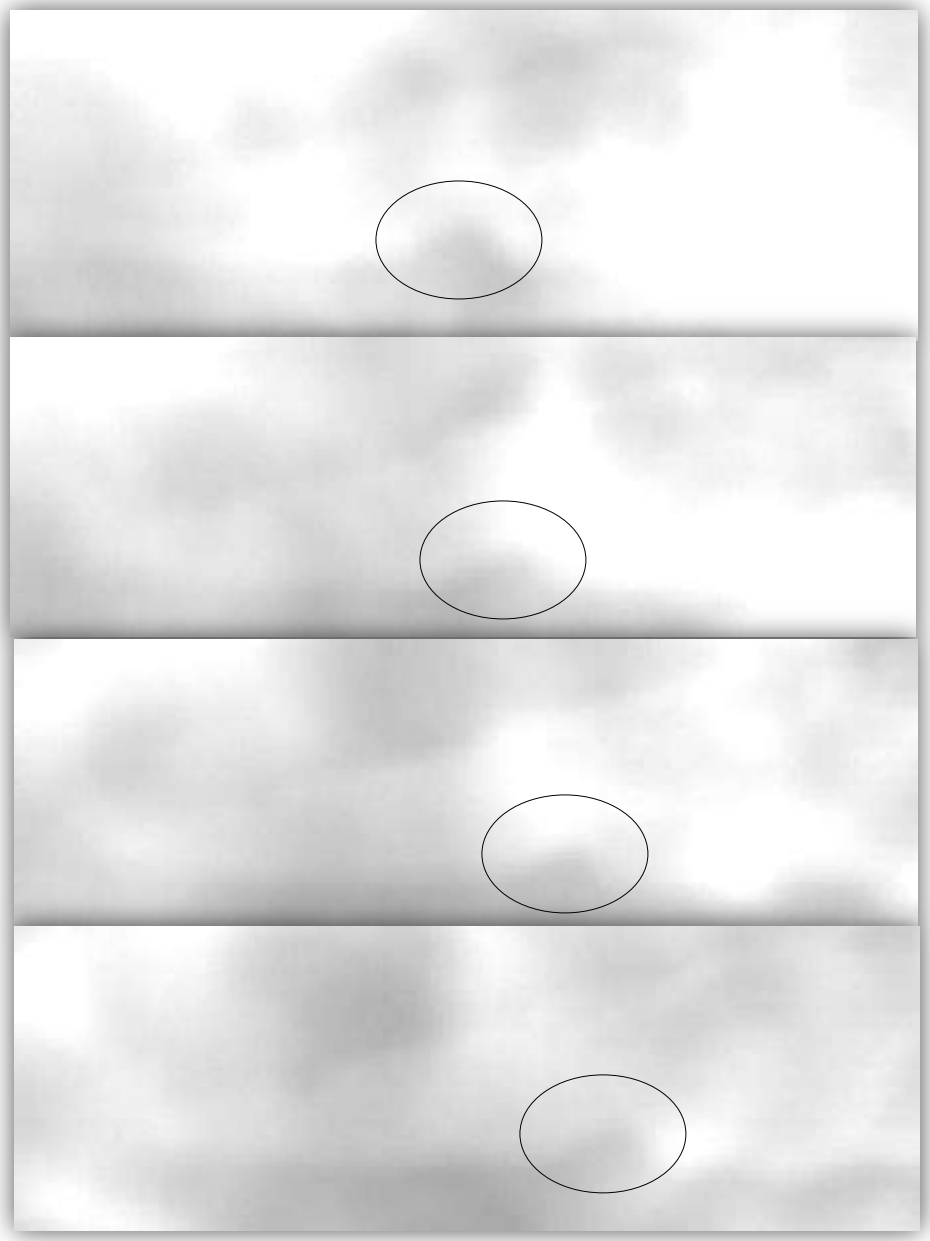

Figure 2.10: The video of Lexan shot three shows a clear plasma jet expansion to the right. The ET source is on the left side of the images. The discontinuity, circled in black, is used to calculate plasma plume velocity.

To measure plasma velocity a reference frame was measured using a ruler at the focal length of the ET source. This reference frame, Figure 2.11, was used to correlate how far the discontinuity moves between frames in the video. The reference frame is 1024x1024 (width x

height) pixels and the Lexan shot three video is 192x128 pixels. The reduction in resolution is due to the increased frame rate of the video versus the single image. In the calibration image 10 ± 1 pixel is equal to 1 mm at the focal length of the camera. This distance is not the same in the plasma video because the pixels are larger. Using equation (5) to solve for (x) returns the corresponding number of pixels equivalent to the calibration image. 192 is the number of pixels in the horizontal of the plasma image, and 1024 is the number of pixels in the horizontal of the calibration image.

$$192(x) = 1024 \tag{5}$$

The images and videos were taken on a level plane to eliminate the need to calculate multiple velocity vector components. Equation (5) simplifies because the focal length, camera sensor, and field of view are constant. 1 pixel in the plasma image is equal to 5.33 pixels in the calibration image. The discontinuity moves 11 ± 2 pixels, and because of the larger pixels in the plasma images this is equal to 58.87 ± 10.87 pixels in the calibration image. The low resolution and out of focus plasma images introduce a large variation in the distance. 10 pixels in the calibration image is 1 mm, so 58.87 pixels correspond to 5.89 mm. The time between each frame is 10 μs at 100,000 fps. The distance and time are known so plasma velocity can be calculated. This process was also completed in the MATLAB® image processing toolbox to compare and obtain more precise calculations.

Figure 2.11: The calibration image, 1024x1024, was taken at the same focal length as the plasma video. The image is used to find the distance traveled by the discontinuity in the plasma video.

Videos and images can be imported into MATLAB®. For this process the calibration image, and the frames used to measure plasma velocity were imported. Figure 2.12 illustrates two consecutive frames from the plasma video spliced together to show how far the discontinuity moves between frames. The first frame, in pink, is on the left, and the second frame, in green, is on the right. In the calibration image 10 pixels equals 1 mm, and the discontinuity in the plasma video moves 10 ± 1 pixels. Using MATLAB® decreased the error in the results. Images can be fused together and pixels can be identified individually making comparing images much easier.

Figure 2.12: MATLAB® was used to fuse frames together so that the distance between the discontinuity in each frame could be measured. Frame one is on the left, and frame two is on the right. This figure does not represent the true distance between images.

Chapter 3: Results and Discussion

This chapter includes results obtained from the spectroscopic and high speed camera data collected on the ET discharge facility PIPE, specifically, electron plasma temperature, electron number density, dissociation of Lexan, and plasma jet velocity. Some interesting things discovered in the analyzed spectra are pointed out, and issues that were discovered during data collection and how these issues were resolved is also discussed.

Many shots were conducted throughout this preliminary research, but few shots revealed video and spectral data that could be used for analysis. Electron plasma temperature was estimated using the relative line method and also from previously compiled tables from plasma simulation. The plasma tables used from (Gigosos and Cardenoso) were generated for use with higher density plasma and are based on the simulation of hydrogen peaks in emission spectra [73]. The estimated temperatures from the 1.485 KJ shot spectrum will be compared to ETFLOW which is the existing code that simulates the PIPE device. Results from this study will be compared to previous simulations of comparable energy. From the tables, electron plasma temperature at the given density is 0.43 eV (4990 K). From the relative line intensity method using copper lines the electron temperature is estimated to be $0.34 \pm 43\%$ eV. ETFLOW returns values of $1.98 \pm 4\%$ eV for similar energy shots [3]. ETFLOW gives a range of values because it calculates values based on an ideal model and non-ideal model ET plasma. The discrepancy in temperature and large uncertainty can be explained by error in the relative line method by choosing the copper lines, or in what stage of formation the temperature measurements are taken. It is possible that the peak intensities of the copper lines are not entirely copper due to impurities in the plasma such as air and chlorine. Also, the spectrum was averaged over a time of one millisecond which will mask certain strong intensity emissions. ETFLOW simulates plasma

temperature only inside the mouth of the source, whereas the temperature measurements estimated from the spectrum come from the expanded region of the plasma jet around an inch away from the source. The plasma jet will rapidly expand, cool, and recombine once it exits the source which explains the drop in electron temperature. Electron density should follow the same trend.

Similarly, density measurements are estimated using the tables as well as the stark broadened H-β line at 486 nm. Measurements are calculated from the same 1.485 KJ Lexan shot. The density estimated from the table, which corresponds to the electron temperature of 0.43 eV, is $4.68*10^{22}$ m^{-3} [73]. Measuring the FWHM of the H-β line in the spectrum estimates electron density to be $5.75*10^{22} \pm 26\%$ m^{-3}. ETFLOW predicts $9*10^{25} \pm 18\%$ m^{-3}right before expansion for shots of this energy [3]. Another study found electron densities of $3*10^{23} – 2*10^{24}$ m^{-3} in the expanded region of the plasma jet of a similar experiment [67]. Estimates from this study are comparable to those of similar experiments on ET devices [8-9]. Both studies show that the electron density drops by many orders of magnitude as the plasma jet expands. Electron density will diminish as elements and molecules in the jet recombine and gain electrons. This is evidenced by the appearance of CN and CO_2 in the spectrum.

In ETFLOW it is assumed that Lexan is fully dissociated. Spectral analysis of the same 1.485 KJ shot can assist in the verification of this assumption. Lexan is a polymer so there are many carbon-carbon bonds mostly due to Benzene (C_6H_6). If multiple carbon linked compounds do not appear in the spectrum of the shot then the full dissociation assumption should be valid. In the Lexan monomer the C=O double bond is the strongest with a bonding energy of 799 KJ/mol and the C=C double bond is the second strongest with 614 KJ/mol [75]. For a shot of this energy the ablated mass of Lexan has been measured to be around 25 mg [3]. Knowing the

molar weight of Lexan, the bonding energies of each bond in Lexan, and the ablated mass of Lexan in the shot, the energy needed to dissociate the Lexan completely can be estimated to be around 1.526 KJ. In the spectrum there is no evidence of Benzene lines or any carbon-carbon bonds larger than C_2. There is no evidence of CO lines indicating that the strongest bond in the Lexan is broken, however the existence of the CN and CO_2 is evidence of recombination. If recombination is occurring and the stronger CO bonds appear to be broken then the C_2 is most likely from recombination in the expansion of the plasma jet.

There is sufficient evidence to say that the full dissociation assumption in ETFLOW is valid. No carbon chains exist in the spectrum, the energy of the shot is close to the energy required for dissociation, and the bonds that may have survived are also possibly from recombination. Keep in mind that Lexan shot two is a lower energy shot at 3.54 KA. Shots made at peak currents at over 40 KA have much higher input energies so Lexan would most definitely be fully dissociated. Knowing that the dissociation assumption in the simulation code is valid is a tremendous validation for this field. Confirming the code allows future code editors to include the assumption in their simulations, and knowing the energy for full dissociation of Lexan can be used by any users of the material in their research or industrial processes.

Other things found in the spectrum that are of interest are chlorine and the ratio of tungsten and zinc. Chlorine was identified in the spectrum. This is because chlorine is used in the manufacture of Lexan when phosgene is chemically reacted with hydrochloric acid. Trace amounts of chlorine from manufacturing will be attached to the end of Lexan chains, and when the Lexan is dissociated ionized chlorine peaks appear in the spectrum. Also the ratio of tungsten to zinc is similar in the spectrum. Remember that the cathode is 70% tungsten and the brass anode is 30% zinc. Unfortunately the lines of these elements matched with other lines of

known elements in the plasma so an attempt to estimate material ablated from the cathode and anode would not be accurate.

The plasma velocity was measured manually and in MATLAB® using a 100,000 fps video from a Lexan shot with a net energy of 2.053 KJ and 17.75 KA. The manual calculations estimated the plasma velocity to be 5867 m/s $\pm$ 1000 m/s. The large error is caused by error in manual calculations and uncertainty in distance in the low resolution images. Using MATLAB® to estimate plasma velocity gave values of 5333 m/s $\pm$ 500 m/s. ETFLOW estimates peak plasma velocity at the exit of the source to be between 5000 and 5300 m/s. The estimates of bulk plasma velocity are in agreement with the code results for similar shots. The velocity measurements in the video are not calculated from the plasma at the exit of the source. Measurements are made using the only identifiable discontinuity in the plasma jet that appears to flow along with the plasma plume. This discontinuity, illustrated in Figure 2.10, is yet unknown in origin. It is possible that is it of supersonic origin or possibly a stable eddy. Mach disks have been examined in ET plasma devices before [60, 66-67]. Given the shape of the chamber and the development of the plasma jet in the video at the time of observation it is possible that backflows or eddy currents form when high pressure plasma hits the wall and recirculates underneath the jet causing the discontinuity. These preliminary velocity measurements on the PIPE device are the first velocity measurements attempted on the device. More measurements will be needed to properly validate the ETFLOW code, but seeing that the preliminary measurements are in agreement with the simulation is a large step forward in the capabilities of experimental measurements in the lab. Attaining these results also validates this method for others using ET discharge devices.

During data collection it was discovered that the continuum of emission from the plasma plume saturates the high resolution spectrometer, which makes it nearly impossible to extract quality data from a spectrum. An example of a saturated spectrum is shown below in Figure 3.1. Most of the lines are clipped off so it is impossible to obtain true line intensities from most of the spectrum. This can be corrected by properly triggering the spectrometer with a delay generator. This corrects the triggering issue and the saturation issue simultaneously. To trigger the LIBS2500plus it must receive a 5 V signal on the "lamp sync" SMA port, and not the "ext trig" port. Also, in the software, "use external triggering DLL", and "continuous laser mode" must be selected for the spectrometer to properly receive a trigger to record and save spectra automatically. By delaying the trigger of the spectrometer the bright continuum flash from the initial plasma plume can be avoided, and the emission lines that appear during the relaxation of the excited plasma can be captured. Having solved these issues will make experimental data collection on ET discharges at Virginia Tech much easier and assist greatly with future work.

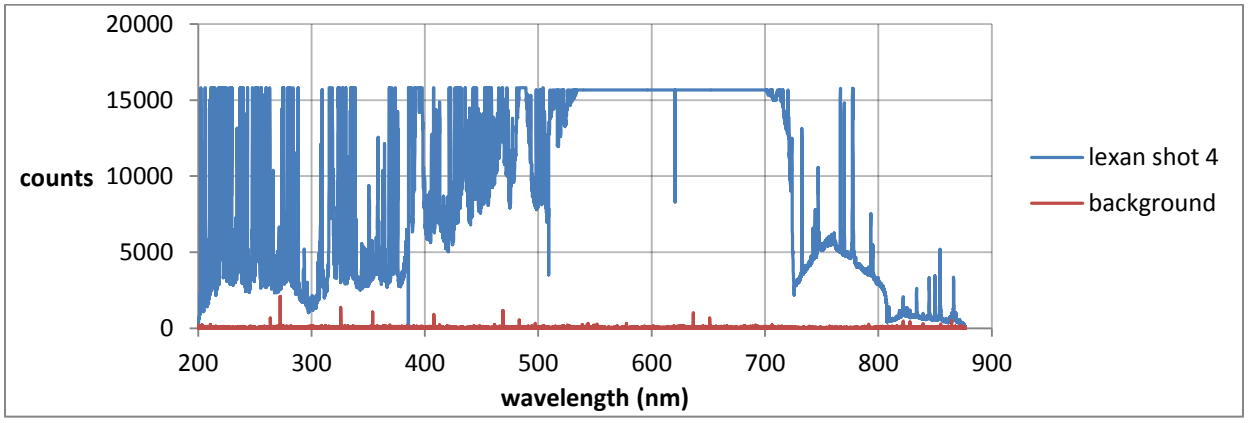

Figure 3.1: Spectrum of Lexan shot four that was saturated by the intense continuum of light emitted from the ET plasma as it forms a plume.

Chapter 4: Conclusions and Future Work

4.1 Conclusion

The purpose of this study was to perform preliminary optical experimental measurements on the PIPE facility to verify ETFLOW results with experimental measurement, the assumption of full dissociation of Lexan in the plasma, and resolve triggering and saturation issues with the high resolution spectrometer. Electron temperature measurements from a 1.485 KJ Lexan shot were estimated to be $0.34 \pm 43\%$ eV where ET flow results predicted $1.98 \pm 4\%$ eV. Electron density estimates from the same shot were $5.75*10^{22} \pm 26\%$ m^{-3}, while ETFLOW predicted $9*10^{25} \pm 18\%$ m^{-3}. Electron temperature and density measurements are within the expected range given that the experimental data was collected in the expanding plasma jet rather than the end of the ET source. Measurements cannot be made inside the source without modifications to the source itself. The temperature and density of the plasma should be smaller as the plasma exits the source and expands and cools. These results show agreement with what is expected in the expansion region of the plasma jet. This helps to validate the usefulness of ETFLOW in simulating these types of discharges. These measurements will be important to validate a new code that is currently under construction to extend ETFLOW's simulation from the source to the plasma jet region. This and future results will be invaluable to validating this new code.

Velocity measurements from the high speed camera agree very well with ETFLOW simulations. 5333 m/s $\pm$ 500 m/s as measured in MATLAB®, and 5000 - 5300 m/s as predicted in ETFLOW. These preliminary measurements not only provide the first validating velocity measurements collected from the PIPE device, but provide Virginia Tech with new capabilities of data collection that were not possible before. Similar to the temperature and density

measurements, the velocity measurements will be used to validate future simulation codes that include plasma jet simulations and not just source simulations. The validation of electrothermal discharge simulations in the expansion region would be extremely useful in all aspects of ET discharge applications including research, hypervelocity launchers, fusion energy, propulsion, and improving combustion efficiencies in engines.

According to spectral analysis there are no large carbon-carbon bonds, the C=C bonds are most likely from recombination, and the energy of the Lexan shot is close to that needed for complete dissociation. The analyzed shot is low energy compared to others in this data set. 1.485 KJ compared to shots around 2.053 KJ. Due to the much larger number of C=C bonds in Lexan compared to C=O bonds it is possible that some C=C bonds could survive to form the Swan Band system seen in the spectrum, but because of the integration period of the shot it is not certain. For a higher energy shot it is certain that Lexan is completely dissociated and for lower energy shots the Lexan is most likely fully dissociated. Verifying this assumption in the ETFLOW code allows future researchers to be sure that the assumption they are using is true. This knowledge will be extremely useful for any research group modeling or experimenting with data collection on ET plasmas involving Lexan and possibly the use of Lexan in industrial processes.

The data collection issues of saturation and triggering of the high resolution spectrometer have been resolved with a combination of new wiring, software settings, and a delay generator. Properly triggering the spectrometer with a delay generator avoids the bright continuum of the plasma jet when it first expands out of the source. This method does not require equipment other than what is already available in the laboratory. Solving these issues is important to future experiments taken on PIPE as well as for the device under construction at Virginia Tech. The

new changes in the data collection configuration will be incorporated into the design of the new ET system to make data collection a more automated and precise process by removing part of the human error. This new configuration along with the high speed camera provides new capabilities in data collection on ET plasma discharge devices not previously attainable in this laboratory.

4.2 Future Work

Many more spectra must be collected and analyzed to compare to the spectrum in this study. A large pool of analyzed spectra will be needed for the simulation validation process. For further characterization of ET plasmas detailed fluorescence mapping of elements in the plasma can reveal number densities of specific elements. It would be of utmost interest to see the amount of material that is ablated off the cathode and anode with each shot. A high flash rate Xenon lamp has been purchased for these experiments. Absorption measurements could also be undertaken to identify molecules in spectra. An ET system is currently under construction to incorporate findings from this study into the design to make data collection easier in the future. Viewports for fluorescent excitation sources and high speed imaging, feedthroughs for fiber optic cables, and specialty triggering circuits to automate the process and obtain time resolved spectra of the ET discharge are planned to be incorporated.

References

[1] V. Narayanaswamy, L.L. Raja, and N. T. Clemens. “Characterization of a High-Frequency Pulsed-Plasma Jet Actuator for Supersonic Flow Control.” AIAA JOURNAL, Vol. 48, No. 2, February 2010.

[2] Dah Y. Cheng. “Electro-thermal Pulsed Fuel Injector and System.” US Patent Number 5165373. Nov 24. 1992.

[3] A. L. Winfrey, et al. “A Study of Plasma Parameters in a Capillary Discharge With Calculations Using Ideal and Nonideal Plasma Models for Comparison With Experiment.” IEEE Transactions on Plasma Science. 2012.

[4] JA Bittencourt. “Fundamentals of Plasma Physics.” New York: Springer-Verlag Inc, 3rd edition, National Institute for Space Research. 2010.

[5] R. W. Kincaid, M. A. Bowham, and J. G. Gilligan. “Pellet Acceleration Using an Ablation-Controlled Electrothermal Launcher.” Proc. 16th IEEE/NPSS Symposium on Fusion Engineering. September 30 1995.

[6] M.Ali Kettani and Max F. Hoyaux. “Plasma Engineering.” New York: Halsted Press Division, John Wiley and Sons. 1973.

[7] The NIST Reference on Constants, Units, and Uncertainty. <http://physics.nist.gov/cuu/index.html?sess=5ae0912162ec5982b566fee56b2c0abd> Accessed on December 21, 2013.

[8] 0. E. Hankins, M. A. Bourham, D. Mann. “Observations of Visible Light Emission from Interactions between an Electrothermal Plasma and a Propellant.” IEEE Transactions on Magnetics, Vol 33, No I. January 1997.

[9] 0. E. Hankins, M. A.. Bourham, J. Earnhart and J. G. Gilligan, "Visible Light Emission Measurements from a Dense Electrothermal Launcher Plasma," IEEE Transactions on Magnetics, Vol. 29, 1158. 1993.

[10] George Odian. "Principals of Polymerization." New York: John Wiley and Sons Inc. 4th edition. 2004.

[11] A. L. Winfrey. "A Numerical Study of the Non-Ideal Behavior, Parameters, and Novel Applications of an Electrothermal Plasma Source." Ph.D. dissertation, Mechanical Engineering NCSU. Raleigh North Carolina, 2010.

[12] American Chemical Society, "THE FOUNDATION OF POLYMER SCIENCE BY HERMANN STAUDINGER (1881-1965)," Freiburg, Baden-Württemberg, April 19, 1999. Accessed on Dec 28, 2013.

[13] J.D. Swift and M.J.R. Schwar. "Electrical Probes for Plasma Diagnostics" New York American Elsevier Publishing Company.

[14] Hans R. Griem. "Principals of Plasma Spectroscopy" Cambridge University Press. 1997.

[15] I.M. Podgornyi. "Topics in Plasma Diagnostics" Plenum Press, New York. 1971

[16] J.P. Sharpe, M. Bourham, J.G. Gilligan. "Generation and Characterization of Carbon Particulate in Disruption Simulations" Department of Nuclear Engineering, NCSU. Fusion Technology Vol. 34, Nov. 1998.

[17] T.E. Gebhart and A.L. Winfrey ; A Computational Study of Lithium Solid Propellants for Magnetic Confinement Fusion Fueling . IEEE Symposium on Fusion Energy Paper ThPO-49; San Francisco CA 11-14 June 2013.

[18] S.K. Murali. “Optical Emission Spectroscopy of Electrothermal Plasmas and Verification of Local Thermodynamic Equilibrium.” Thesis. Deaprtment of Nuclear Engineering, North Carolina State University, Raleigh. 1998.

[19] T.E. Gebhart. “A Computational Study of a Lithium Deuteride Fueled Electrothermal Plasma Mass Accelerator” Thesis. Deaprtment of Mechanical Engineering, Virginia Polytechnic Institute and State University, Balcksburg. 2013.

[20] J.P. Sharpe, M.A. Bourham, J.G. Gilligan. “Generation and Characterization of Carbon Particulate in Disruption Simulations.” Fusion Technology, Vol. 34, pp. 634 – 639, Nov. 1998.

[21] D.J. Griffiths. “Introduction to Electrodynamics.” New Jersey: Prentice-Hall, Inc. 3rd edition, 1999.

[22] Min-Hyong Lee, Sung-Ho Jang, and Chin-Wook Chung. “Floating probe for electron temperature and ion density measurement applicable to processing plasmas.” Journal of Applied Physics: Online February 13, 2007.

[23] Patrick Nguyen Huu. “Langmuir Probe Diagnostics on the LEAP Electrothermal Thruster.” Perdue University: Masters Thesis in Aeronautics and Astronautics. West Lafayette Indiana. May 2010

[24] M. Takeshi, et al. “Optical Measurements of Exhaust Process of an Electrothermal Pulsed Plasma Thruster.” Transactions of Joining and Welding Research Institute (JWRI), Vol 41, 2012.

[25] K. Kadota, et al. “Plasma Diagnostics by Neutral Beam Probing.” Institute of Plasma Phyiscs: Nagoya University, Japan. Vol. 20, April 1978.

[26] R. J. Fonck, P. A. Duperrex, and S. F. Paul. “Plasma Fluctuation Measurements in Tokamaks Using beam-plasma Interactions.” American Institute of Physics, Vol 61, November 1990.

[27] E. P. Muntz, F. M. Lufty, and I. D. Boyd. “The Study of Reacting, High Energy Flows Using Pulsed Electron-Beam Fluorescence.” 27th AIAA Fluid Dynamics, Plasma Dynamics, and Laser Conference, June 1996.

[28] R. J. Chaffin and J. B. Beyer. “Plasma Diagnostics with a Microwave Fabry-Perot Resonator.” IEEE transactions on microwave theory and techniques, Vol. MTT-16, No. 1, January 1968.

[29] H. J. Hartfuss. “Fusion Plasma Diagnostics with Microwaves.” Max-Planck Institute, Germany. IEEE conference proceedings. September 2010.

[30] M. N. Shneider and R. B. Miles. “Microwave Diagnostics of Small Plasma Objects.” Princeton University. Journal of Applied Physics, August 2005.

[31] R. L. Stenzel and R. W. Gould. “Afterglow Plasma Diagnostics with a Microwave Sampling Radiometer.” California Institute of Technology. The Review of Scientific instruments, Vol. 40, No. 11, November 1969.

[32] A. Brockhaus, et al. “Electron Density Measurements in a Microwave Plasma by the Plasma Oscillation Method.” University of Wuppertal Germany.

[33] J. Yang, et al. “Development and Research of a Coaxial Microwave Plasma Thruster.” Review of Scientific Instruments, Vol. 79, August 2008.

[34] Y. Takao, et al. “Plasma Diagnostics and Thruster Performance Analysis of a Microwave-Excited Microplasma Thruster.” Japanese Journal of Applied Physics, Vol. 45, No. 10B, 2006.

[35] M. C. Hawley, et al. “Review of Research and Development of the Microwave Electrothermal Thruster.” American Institute of Aeronautics and Astronautics (AIAA), Vol. 5, No. 6, November 1989.

[36] W. McColl, et al. “Electron Density and Collision Frequency of Microwave-Resonant-Cavity-Produced Discharges.” American Institute of Physics. Vol. 74, No. 6, September 1993.

[37] J. W. Rogers, et al. “An Experiment to Measure the Mass Density of a Plasma Armature.” IEEE Transactions on Magnetics, Vol. 27, no. 1, January 1991.

[38] P. Tran, et al. “Relationship Between Plasma Energy and Gas Generation in an Electrothermal-Chemical Gun.” Army Research Laboratory. January 1994.

[39] P. Klein and D. Meiners. “Measurement of Width and Shift of Rare Gas Lines Emitted From a Shock Tube Plasma.” Journal on Quantitave Spectroscopy and Radiation Transfer. Vol. 17, Pg 197, June 1976.

[40] J. L. Wilson, et al. “Plasma Flow in an Electromagnetic Shock Tube and in a Compression Shock Tube.” Ministry of Aviation, Aeronautical Research Council. No. 886, 1966.

[41] N. Hershkowitz and Y. C. Ghim. “Probing Plasmas with Ion Acoustic Waves.” Plasma Sources Science and Technology. Vol. 17, August 2008.

[42] A. Brown. “Ion Acoustic Waves.” Duke University. March 5, 2007.

[43] S. H. Glenzer, et al. “Observation of Two Ion-Acoustic Waves in a Two-Species Laser-Produced Plasma with Thomson Scattering.” American Physical Society. Vol. 77, No. 8, August 19, 1996.

[44] V. Margetic, et al. “A Comparison of Nanosecond and Femtosecond Laser-Induced Plasma Spectroscopy of Brass Samples.” Institute of Spectrochemistry and applied Spectroscopy, Germany. Spectrochimica Acta, Vol. 55, May 2000.

[45] A. W. Miziolek, et al. “Laser-Induced Breakdown Spectroscopy (LIBS): Fundamentals and Applications.” Cambridge University Press. August 2008.

[46] R. Ahmed and M. A. Baig. “A Comparative Study of Single and Double Pulse Laser Induced Breakdown Spectroscopy.” Atomic and Molecular Physics Laboratory, Pakistan. Journal of Applied Physics, Vol. 106, 2009.

[47] E. Thomas Jr. “Direct Measurements of Two-Dimensional Velocity Profiles in Direct Current Glow Discharge Dusty Plasmas.” American Institute of Physics. Physics of Plasmas. Vol. 6, No. 7, 1999.

[48] E. Thomas Jr., J. D. Williams, J. Silver. “Application of Stereoscopic Particle Image Velocimetry to Studies of Transport in a Dusty (Complex) Plasma.” American Institute of Physics. Physics of Plasmas. Vol. 11, No. 7, July 2004.

[49] L. Boufendi, et al. “Particle-Particle Interactions in Dusty Plasamas.” American Institute of Physics. Journal of Applied Physics. Vol. 73, 1993.

[50] P. Clancy, J. H. Kim, M. Samimy. “Planar Doppler Velocimetry in High Speed Flows.” American Institute of Aeronautics and Astronautics, Fluid Dynamics Conference, 27th, June 1996.

[51] R. J. Adrian. “Strategies for Imaging Flow Fields with Velocimetry.” American Institute of Aeronautics and Astronautics, Fluid Dynamics Conference, 27th, June 1996.

[52] G. E. Elsinga, et al. “Tomographic Particle Image Velocimetry.” Springer-Verlag, Experiments in Fluids, 2006.

[53] Dr. Phillip J. W. Roberts. "Hydrodynamics of Initial Mixing Zones of Wastewater Discharges." Georgia Institute of Technology. EPA, November 2001.

[54] R. M. Cothren, et al. "Detection of Dysplasia at Colonoscopy Using Laser-Induced Fluorescence: A Blinded Study." American Society of Gastrointestinal Endoscopy. Vol. 44, No. 2, 1996.

[55] R. Teichmann, et al. "Applications of the LIF Method for the Diagnostics of the Combustion Process of Gas-IC-Engines." Springer: Combustion Engines Development. Vol. 25, 2012.

[56] Cheng, Dah. "Electro-thermal Pulsed Fuel Injector and System." patent 5165373. Nov. 22, 1992.

[57] S. E. Parrish, R. J. Zink. "Development and Application of a High-Speed Planar Laser-Induced Fluorescence Imaging System to Evaluate Liquid and Vapor Phases of Sprays From a Multi-Hole Diesel Fuel Injector." General Motors. Measurement Science and Technology. Vol. 24, 2013.

[58] J. P. Booth, et al. "Spatially and Temporally Resolved Laser Induced Fluorescence Measurements of CF2 and CF Radicals in a CF4 rf Plasma." Journal of Applied Physics. Vol. 66, 1989.

[59] F. M. Levinton and F. Trintchouk. "Visualization of Plasma Turbulence with Laser Induced Fluorescence." American Institute of Physics. Review of Scientific Instruments, Vol. 72, 2001.

[60] J. U. Kim, Y. J. Kim, and B. Hong. "Planar Laser-Induced Fluorescence (PLIF) Measurements of a Pulsed Electrothermal Plasma Jet." KSME International Journal. Vol. 15, No. 12, 2001.

[61] M. D. Ryan, N. T. Clemens, and P. L. Varghese. “Experimental Investigation of the Interaction of Electrothermal Plasmas with Solid Propellants.” AIAA 42nd Aerospace Sciences Meeting and Exhibit. January 2004.

[62] M. D. Ryan, N. T. Clemens, and P. L. Varghese. “Spectroscopic Measurements During an Electrothermal Plasma-JA2 Solid Propellant Interaction.” AIAA 44th Aerospace Sciences Meeting and Exhibit. January 2006.

[63] J. U. Kim and H. Suk. “Characterization of a High-Density Plasma Produced by Electrothermal Capillary Discharge.” American institute of Physics. Applied Physics Letters, Vol. 80, No. 3, 2002.

[64] B. Brill, et al. “Density Measurement of Dense Capillary Discharge Plasma Using Soft X-Ray Backlighting.” Journal of Physics D: Applied Physics. Vol. 23, No. 8, 1990.

[65] C. Charles, et al. “Nanosecond Optical Imaging Spectroscopy of an Electrothermal Radiofrequency Plasma Thruster Plume.” Applied Physics Letters, Vol. 103, No. 12, September 2013.

[66] W. A. Page. “A Survey of Thermal Radiation Studies of Ablating Bodies in the Ballistic Range.” NASA Technical Note. Ames Research Center. 1967.

[67] J. M. Kohel, et al. “Emission Spectroscopic Measurements and Analysis of a Pulsed Plasma Jet.” IEEE Transactions on Magnetics, Vol. 35, No. 1, January 1999.

[68] K. J. White, et al. “Plasma Characterization for Electrothermal-Chemical (ETC) Gun Applications.” Army Research Laboratory: Aberdeen Proving Grounds. September 1997.

[69] J. Gilligan, et al. “Studies to Reduce Material Erosion in Electrothermal Launchers.” IEEE Transactions on Magnetics, Vol. 27, No. 1, January 1991.

[70] J. Sharp. “Plasma Monitoring with the HR2000+ High Resolution Spectrometer.” Ocean Optics Plasma Monitoring Article. May 2012.

[71] Ocean Optics Inc. “Laser-Induced Breakdown Spectroscopy LIBS2500plus: Installation and Operation Manual.” 830 Douglas Ave., Dunedin FL. 2010.

[72] J.E. Sansonetti and W. C. Martin. “Handbook of Basic Atomic Spectroscopic Data.” NIST. American Institute of Physics, September 28, 2005.

[73] M. A. Gigosos and V. Cardenoso. “New Plasma Diagnosis Tables of Hydrogen Stark Broadening Including Ion Dynamics.” Journal of Physics B: Atomic, Molecular and Optical Physics. Vol. 29, pg 4795-4838. 1996.

[74] B. Pajot. “Optical Absorption of Impurities and Defects in Semiconducting Crystals.” Springer Series in Solid State Sciences. Pg 86. 2010.

[75] Brown, LeMay, and Bursten. “Chemistry: The Central Science.” Prentice-Hall, Inc. 8th edition. 2000.